

Time-reversal method and cross-correlation techniques by normal mode theory: a three-point problem

M Montagner, M Larmat, M Capdeville, E Fink, H Phung, B. Romanowicz, E Clévédé, H Kawakatsu

▶ **To cite this version:**

M Montagner, M Larmat, M Capdeville, E Fink, H Phung, et al.. Time-reversal method and cross-correlation techniques by normal mode theory: a three-point problem. Geophysical Journal International, 2012, 191 (2), pp.637-652. 10.1111/j.1365-246X.2012.05619.x . insu-01397671

HAL Id: insu-01397671
https://insu.hal.science/insu-01397671

Submitted on 16 Nov 2016

HAL is a multi-disciplinary open access archive for the deposit and dissemination of scientific research documents, whether they are published or not. The documents may come from teaching and research institutions in France or abroad, or from public or private research centers.

L'archive ouverte pluridisciplinaire **HAL**, est destinée au dépôt et à la diffusion de documents scientifiques de niveau recherche, publiés ou non, émanant des établissements d'enseignement et de recherche français ou étrangers, des laboratoires publics ou privés.

Geophysical Journal International

Geophys. J. Int. (2012) **191,** 637–652 doi: 10.1111/j.1365-246X.2012.05619.x

Time-reversal method and cross-correlation techniques by normal mode theory: a three-point problem

J.-P. Montagner,[1] C. Larmat,[2] Y. Capdeville,[1] M. Fink,[3] H. Phung,[1] B. Romanowicz,[4] E. Clévédé[1] and H. Kawakatsu[5]

[1]*Seismology Laboratory, Institut de Physique du Globe UMR-CNRS* 7154, 1 *rue Jussieu* 75238 *Paris Cedex* 05, *France. E-mail: jpm@ipgp.fr*
[2]*L.A.N.L., Los Alamos, NM, USA*
[3]*Institut Langevin, ESPCI ParisTech, CNRS,* 1 *rue Jussieu,* 75005 *Paris, France*
[4]*Seismology Lab., U.C. Berkeley, Berkeley, CA, USA*
[5]*Earthquake Research Institute, University of Tokyo, Japan*

Accepted 2012 July 20. Received 2012 July 10; in original form 2011 December 20

SUMMARY

Since its beginning in acoustics, the Time-Reversal method (hereafter referred as TR) has been explored by different studies to locate and characterize seismic sources in elastic media. But few authors have proposed an analytical analysis of the method, especially in the case of an elastic medium and for a finite body such as the Earth. In this paper, we use a normal mode approach (for general 3-D case and degenerate modes in 1-D reference model) to investigate the convergence properties of the TR method. We first investigate a three-point problem, with two fixed points which are the source and the receiver and a third one corresponding to a changing observation point. We extend the problem of a single channel TR experiment to a multiple channel and multiple station TR experiment. We show as well how this problem relates to the retrieval of Green's function with a multiple source cross-correlation and also the differences between TR method and cross-correlation techniques. Since most of the noise sources are located close to the surface of the Earth, we show that the time derivative of the cross-correlation of long-period seismograms with multiple sources at the surface is different from the Green's function. Next, we show the importance of a correct surface-area weighting of the signal resent by the stations according to a Voronoi tessellation of the Earth surface. We use arguments based on the stationary phase approximation to argue that phase-information is more important than amplitude information for getting a good focusing in TR experiment. Finally, by using linear relationships between the time-reversed displacement (resp. strain wavefields) and the components of a vector force source (resp. a moment tensor source), we show how to retrieve force (or moment tensor components) of any long period tectonic or environmental sources by time reversal.

Key words: Time series analysis; Numerical solutions; Interferometry; Earthquake source observations; Surface wave and free oscillations; Theoretical seismology.

Downloaded from http://gji.oxfordjournals.org/ at INIST-CNRS on October 28, 2016

1 INTRODUCTION

Since its first applications in pure acoustics, the time-reversal approach (Fink 1997), has been extended to the 3-D elastic case. A review of some of the current applications for material testing and seismic sources detection can be found in Fink *et al.* (2002), Anderson *et al.* (2008) or Larmat *et al.* (2010). Eigenmode analysis has been used in the scalar case to investigate the limitation of TR in chaotic cavities (Draeger & Fink 1997, 1999) and for diffuse wavefields (Weaver & Lobkis 2002). In this paper, we extend this approach using the normal mode theory for the 3-D elastic Earth. Normal mode theory is very convenient for addressing any scientific issue related to the global scale, since any displacement at the surface of the Earth can be expanded on the basis of normal mode eigenfunctions.

The potential applications in seismology of the TR technique are ongoing for a 3-D elastic Earth. Larmat *et al.* (2006) showed that, when applied to the data of 2004 December 26 Sumatra-Andaman earthquake data, back-propagated waves focused at the right location and the right origin time of the epicentre, and made it possible to retrieve the source-time function, by using a simple normal mode summation code (Capdeville 2005) in a 1-D Earth model such as PREM (Dziewonski & Anderson 1981) at periods larger than 100s. Since then, the method has been implemented in 3-D-heterogeneous models and has been applied to locate glacial earthquakes (Larmat *et al.* 2008), or tremors

© 2012 The Authors
Geophysical Journal International © 2012 RAS

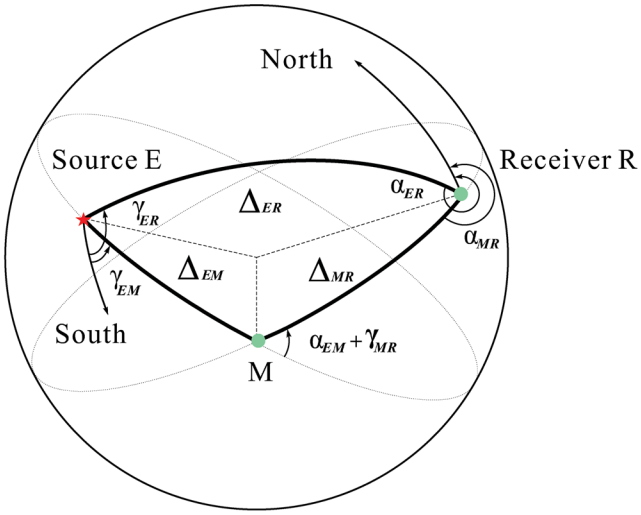


Figure 1. Earthquake epicentre E- receiver R geometry. M is the observation point of the time-reversed wavefield.

(Larmat *et al.* 2009). The potentials and limitations of the time-reversal imaging for finite seismic sources has been explored by Kremers *et al.* (2011). Other potential applications are the location of other environmental sources at global or regional scales, such as the seismic hum (Kobayashi & Nishida 1998; Suda *et al.* 1998; Tanimoto *et al.* 1998; Fukao *et al.* 2002) or long-period volcanic events (O'Brien *et al.* 2011).

It was noted by Draeger & Fink (1999) and then by Derode *et al.* (2003) that the cross-correlation of the signal recorded at two stations, R and M, produced by a source at E, is the same as the time-reversed signal produced in M, when sending back the signal recorded at E produced by a source in R. The similarities and the differences between the TR technique as implemented at the global scale by Larmat *et al.* (2006) and cross-correlation techniques popularized in seismology by Shapiro *et al.* (2005), are explored in this paper by means of the normal mode theory.

The time-reversal method (TRM) is also strongly linked to the adjoint method (see e.g. Tarantola 1988) recently detailed in Tromp *et al.* (2005) as it can be described as the first step of a source location adjoint inversion (Kim *et al.* 2011) with starting seismograms equal to zero. This fact motivates us to explore the link between the time-reversed field and the inversion of the source properties. We derive linear relationships between the time-reversed displacement (or strain wavefields) and the components of a vector force source (or a moment tensor source, respectively) (Kawakatsu & Montagner 2008; Kim *et al.* 2011). The different elements of the related matrices using normal mode summation are derived. These expressions are the first ingredient of a future inversion scheme based on those linear relationships.

Section 2 is a normal mode analysis of a three-point problem which corresponds to a single source TR configuration. In Section 3, we extend the derivations to the cases of a multiple station TR experiment, and of a random distribution of seismic sources. Finally, in Section 4, specific cases of seismic TR are presented. We show that the three-components of elastic waves can be optimally sent back using a correct weighting of station contributions, for the spatio-temporal localization of earthquakes. We use some basic results found in normal mode seismology to confirm the importance of phase information for TR. Finally, we propose a theoretical set-up for recovering the whole seismic force system and moment tensor.

2 TIME REVERSAL WITH NORMAL MODE THEORY

We consider the geometrical situation illustrated in Fig. 1, for the three following points. $E(\theta_E, \phi_E)$ is the source point, $R(\theta_R, \phi_R)$ is the receiver point for the forward problem. $M(\theta_M, \phi_M)$ is a changing observation point that will be needed in the next section.

2.1 Single station time reversal

In this three point problem, E, R, M, the time-reversed signal will be successively calculated at any point M at the surface of the Earth and then, as a particular case, at point E (where $M = E$). Since the problem is linear, the time-reversed field at any point M due to a distribution of receivers can be calculated and will be addressed in the Section 3.1. This kind of calculation can also be used to understand the cross-correlation of noise signals at two different stations (see Section 3.2). This correspondence between cross-correlation and time reversal was already noted in several papers since Draeger & Fink (1999) (see e.g. Derode *et al.* 2003). But this property has been primarily used so far in seismology to get the Green's function (and tensor) between two points, not for studying the seismic sources. For the same reason as for the effect of station distribution on time-reversed field, the effect of a random distribution of sources can be calculated for cross-correlation techniques (see Section 3.2).

At the receiver point $\mathbf{r}_{\mathrm{R}}$, the signal is the result of the convolution of the Green's function with the source time function $(\mathbf{G}_{ER} * \mathbf{f})(t)$. The time reversed seismogram at point $\mathbf{r}_R$ is $(\mathbf{G}_{ER} * \mathbf{f})(-t)$ and in point $\mathbf{r}_M$ the wavefield $\mathbf{S}(\mathbf{r}_M, t)$ will be

$$\mathbf{S}(\mathbf{r}_M, t) = \mathbf{G}_{RM}(t) * (\mathbf{G}_{ER} * \mathbf{f})(-t). \quad (1)$$

Downloaded from http://gji.oxfordjournals.org/ at INIST-CNRS on October 28, 2016

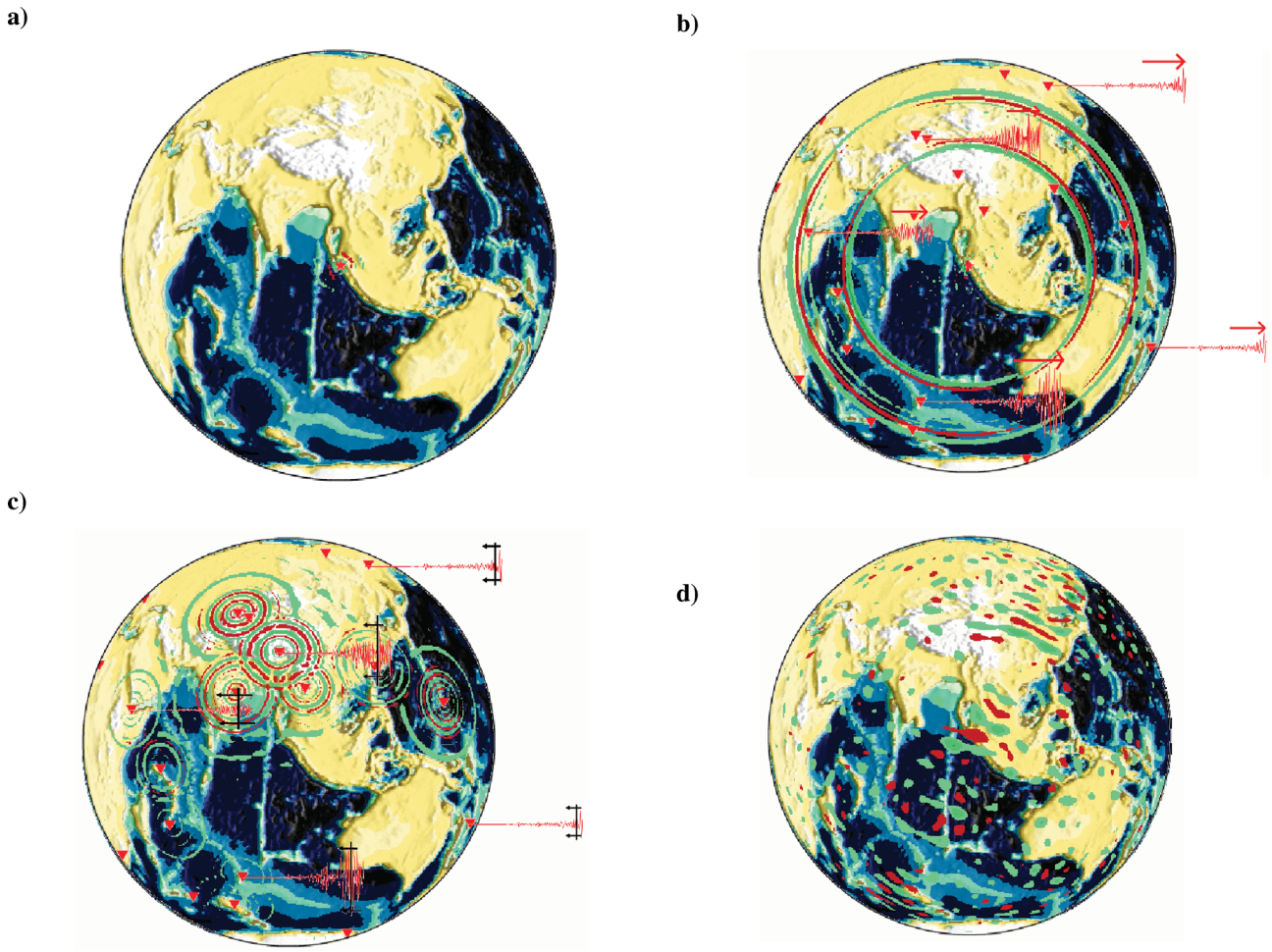


Figure 2. Description of a TR experiment: (a) Earthquake occurrence and forward wave propagation. (b) Recording of seismic wavefield in receivers (red triangles), with some examples of seismograms. (c) Time-reversal broadcast. Each receiver is now a source emitting time-reversed wavefield. (d) Wave back-propagation.

If the source time function is close to a Dirac and due to reciprocity, $\mathbf{S}(\mathbf{r}_M, t) = \mathbf{G}_{RM}(t) * \mathbf{G}_{ER}(-t) = \mathbf{G}_{RM}(t) \otimes \mathbf{G}_{RE}(t)$, the second term being the cross-correlation of the two Green's functions produced by a source at R and recorded, respectively at E and M. As already noted by Draeger & Fink (1999) for scalar eigenmodes, the signal at point E is the autocorrelation function of $\mathbf{G}_{ER}$ which is maximum at $t = 0$.

A TR source location experiment can be described as follows (Fig. 2): first, an earthquake occurs at an unknown point E. The displacement field, $\mathbf{u}(\mathbf{r_R}, t)$, is recorded at a well located receiver position. The recorded time-series is time-reversed (meaning the time-axis is reversed) and is sent from the receiver position into a numerical Earth model.[1] During the re-broadcast, an approximate time-reversed movie of the original wave-propagation will be produced, according to the spatial reciprocity of the wave equation without attenuation. The time-reversed waves will focus back to the source point, allowing its location as well as the retrieval of some source characteristics (Larmat *et al.* 2006; Anderson *et al.* 2008; Larmat *et al.* 2008, 2009; Kim *et al.* 2011). The signal which is sent back is proportional to the displacement limited to the receiver point R. Following a suggestion by McMechan (1982), some first attempts have been done for example in the acoustic case and 2-D medium by McMechan *et al.* (1985), in a 3-D medium for local studies by Gajewski & Tessmer (2005), and for the general elastic case by Larmat *et al.* (2006) at the global scale, by Larmat *et al.* (2008) at the regional scale.

For the elastic case, in a finite body such as the Earth, the displacement solution of the elasto-dynamics equation $\mathbf{u}_{\mathrm{R}}(t)$ can be expanded into the set of eigenmodes $\mathbf{u}_K(r_R, t) = |\mathbf{K}\rangle e^{-\mathrm{i}\omega_K t}$, where ω_K are the eigenfrequencies and $|\mathbf{K}\rangle$ the eigenfunctions according to the Bra-Ket notation of quantum mechanics introduced by P. Dirac (see Cohen-Tannoudji *et al.* 1973). The different notations are explained in Appendix A. In the frequency domain, for a point source in space and time $[\mathbf{F_0}(\mathbf{r}, \omega) = \mathbf{F}_{\mathrm{E}}\delta(\mathbf{r} - \mathbf{r}_{\mathrm{E}})]$, the displacement field $\mathbf{u}_{\mathrm{R}}(\omega)$ recorded at the

[1] In the following derivations, we use the same Green's function with attenuation of the PREM model for the forward and the time-reversed propagation, meaning that the exactly same medium is assumed for both.

Downloaded from http://gji.oxfordjournals.org/ at INIST-CNRS on October 28,

receiver R during the forward propagation is given by the equation (Gilbert 1971)

$$\mathbf{u_R}(\omega) = \sum_K \left(\int_{V_E} dV \mathbf{u}^\dagger_\mathbf{K}(\mathbf{r_E}) \mathbf{F}(\mathbf{r_E}, \omega) \right) \frac{\mathbf{u_K}(\mathbf{r_R})}{-\omega^2 + \omega_K^2} = \sum_K |\mathbf{K_R}\rangle \langle \mathbf{K_E} | \mathbf{F_E}(\omega) \rangle \frac{1}{-\omega^2 + \omega_K^2}, \tag{2}$$

where we note $|\mathbf{K_E}\rangle = \mathbf{u_K}(\mathbf{r_E})\delta(\mathbf{r} - \mathbf{r_E})$, $|\mathbf{K_R}\rangle = \mathbf{u_K}(\mathbf{r_R})\delta(\mathbf{r} - \mathbf{r_R})$ and

$$\mathbf{G_{ER}}(\omega) = \sum_K \frac{|\mathbf{K_R}\rangle \langle \mathbf{K_E}}{-\omega^2 + \omega_K^2} \tag{3}$$

is the Green's function between points E and R. The displacement $\mathbf{u}_\mathrm{R}(\omega)$ is time-reversed, sent back from R and recorded now at the point M as the time-reversed wavefield. The expression of $S_M(\omega)$, the time reversed signal in the Fourier domain, is found by considering the displacement $\mathbf{u}_\mathrm{R}(\omega)$ recorded during the forward propagation.

$$\mathbf{S}_M(\omega) = \sum_J |\mathbf{J_M}\rangle \langle \mathbf{J_R}|\, \mathbf{u}_R(\omega) \delta(\mathbf{r} - \mathbf{r_R}) \frac{\mathbf{1}}{(-\omega^2 + \omega_\mathbf{J}^2)} \tag{4}$$

Following the approach of Capdeville (2005), the contribution of modes J and K, and more importantly, the contributions of the different parts of the path from E to M are separated.

$$\mathbf{S}_M(\omega) = \underbrace{\sum_J \frac{|\mathbf{J_M}\rangle \langle \mathbf{J_R}|}{(-\omega^2 + \omega_J^2)}}_{\mathbf{G}_{RM}(\omega)} \underbrace{\sum_K \frac{|\mathbf{K_R}\rangle \langle \mathbf{K_E}|\mathbf{F_E}\rangle}{(-\omega^2 + \omega_K^2)}}_{\mathbf{C}_{ER}(\omega)} \tag{5}$$

For sake of simplicity, the calculation has been done by assuming that the source time function at point E is a delta function. The generalization to a finite source is easy by using the corresponding source function spectrum instead of a delta function. The case of a source Heaviside function at point E was derived by Gilbert (1971) and is given in eq. (A16). Since the sums over J and K have been separated, and the spectrum of the time-reversed field $\mathbf{S}_\mathrm{M}$ is the product of the spectra of two Green's related functions $\mathbf{G}_{RM}$ and $\mathbf{C}_{ER}$ (convolution of $\mathbf{G}_{ER}$ by $\mathbf{F}_E$), the field in the time domain is the convolution of these two functions. Eq. (5) shows that $\mathbf{G}_{RM}(\omega) = \mathbf{G}_{RM}(-\omega)$ and $\mathbf{C}_{ER}(\omega) = \mathbf{C}_{ER}(-\omega)$. Since the Fourier transform of a time reversed function $f(-t)$ is $F^\star(-\omega)$, and since the cross-correlation of two signals is the convolution of one signal with the other being time–reversed, $\mathbf{S}_\mathrm{M}(t)$ can be computed as expected from eq. (1) as the cross-correlation in the time domain of the two real functions $G_{RM}(t)$ and $C_{ER}(t)$

$$\mathbf{G}_{RM}(t) = \sum_J |\mathbf{J_M}\rangle \langle \mathbf{J_R}| \frac{\sin \omega_J t}{\omega_J} H(t) \tag{6}$$

$$\mathbf{C}_{ER}(t) = \sum_K |\mathbf{K_R}\rangle \langle \mathbf{K_E}|\mathbf{F_E}\rangle \frac{\sin \omega_K t}{\omega_K} H(t). \tag{7}$$

Finally, the time-reversed field is calculated for time duration $\Delta\tau = t_2 - t_1$ between times t_2, and t_1,

$$\mathbf{S}_M(t) = \mathbf{G}_{RM}(t) * \mathbf{C}_{ER}(-t) = \sum_J \sum_K |\mathbf{J_M}\rangle \langle \mathbf{J_R}|\mathbf{K_R}\rangle \frac{\langle \mathbf{K_E}|\mathbf{F_E}\rangle}{\omega_K \omega_J} \underbrace{\int_{t_1}^{t_2} d\tau \, \sin(\omega_J \tau) \sin[\omega_K(t+\tau)]}_{\Im_{JK}(t)}. \tag{8}$$

Eq. (8) might have been directly derived from eq. (1) but the calculation in the Fourier domain illustrates more clearly the passage from convolution to cross-correlation with normal mode formalism. It has the interesting property that it represents the contribution of one receiver and it can be easily generalized to a complete global distribution of receivers (and earthquakes) as will be seen in Section 3.

2.2 Calculation of $\Im_{JK}(t)$

$$\Im_{JK}(t) = \int_{t_1}^{t_2} d\tau \sin[\omega_K(t+\tau)] \sin(\omega_J \tau) \tag{9}$$

$$\Im_{JK}(t) = \frac{1}{2} \sin \omega_K t \int_{t_1}^{t_2} d\tau [\sin(\omega_K + \omega_J)\tau - \sin(\omega_K - \omega_j)\tau] + \frac{1}{2} \cos \omega_K t \int_{t_1}^{t_2} d\tau [\cos(\omega_K - \omega_J)\tau - \cos(\omega_K + \omega_J)\tau].$$

The terms with $(\omega_J + \omega_K)\tau$ are negligible since $1/(\omega_J + \omega_K) \ll \Delta\tau$, provided that the time-series considered is much longer than the longest period in the record. The integrals are different according to the respective values of ω_K and ω_J.

$$\begin{cases} \Im_{JK} = \dfrac{1}{2} \Delta\tau \cos \omega_K t & \text{if } \omega_K = \omega_J \\ \Im_{JK} = \dfrac{1}{2} \dfrac{\sin \omega_K t}{\omega_K - \omega_J} [\cos(\omega_K - \omega_J)t_2 - \cos(\omega_K - \omega_J)t_1] & \text{if } \omega_K \neq \omega_J \\ \qquad + \dfrac{1}{2} \dfrac{\cos \omega_K t}{\omega_K - \omega_J} [\sin(\omega_K - \omega_J)t_2 - \sin(\omega_K - \omega_J)t_1] \end{cases} \tag{10}$$

Downloaded from http://gji.oxfordjournals.org/ at INIST-CNRS on October 28, 2016

The first term is dominant if $\Delta\tau$ is long enough. The second term (when $\omega_K \neq \omega_J$) is more problematic since it can be important when the difference $\omega_K - \omega_J$ is small. The time $\frac{1}{\Delta\omega}$ corresponds to the Heisenberg time. In a chaotic body where modes are non-degenerate, the frequency distribution of ω_K can be considered as random, and the only constructive interference of the sum of modes can be expected for time t around 0 and at point E. The amplitude at the focusing point is proportional to $\Delta\tau$, which means that time reversal experiment incorporates more and more the complexity of the medium. The real Earth, due to 3-D elastic and anelastic heterogeneities and rotation can be considered as such a chaotic body where modes are not degenerate. The Heisenberg time can be extremely long (several tens of thousands seconds), and the rotation necessitates special attention since its effect is not symmetric with respect to time reversal. An interesting result is that we are theoretically able to retrieve the location of the event at the right time and the right location with only one receiver.

However, from a practical point of view, we are unable to calculate the general 3-D Earth normal modes. In the long-period range used in this paper ($100 < T < 1000$ s), the effect of heterogeneities is small, and the Spherically symmetric Non-Rotating Elastic Isotropic (SNREI) model is a good approximation. In that case, the eigenfrequencies are degenerate and only depend on two quantum numbers n, ℓ. In the degenerate case (see Section 2.3), $\frac{1}{\Delta\omega} \approx 2.10^3$ s for eigenperiods around 200 s. It means that if $\Delta\tau \gg \frac{1}{\Delta\omega}$, the non-diagonal terms of $\Im_{JK}$ will tend to interfere destructively and the contribution of non-diagonal terms will be small compared to the diagonal contributions.That is only a zeroth-order approximation valid at very long periods.

If a 3-D heterogeneous Earth model, with non-degenerate modes, could be used for modelling periods shorter than 100s, it should be necessary to use much longer records up to several days. The TRM will work provided that the synthetic Green's function is accurate enough.The expressions given in (10) make it possible to incorporate the coupling between different modes, but this study is beyond the scope of this paper (see e.g. Woodhouse 1980; Capdeville *et al.* 2000; Clévédé *et al.* 2000; Romanowicz *et al.* 2008, for complete discussions of such a coupling). This simple theory can also be extended to the anelastic case by replacing the real eigenfrequencies ω_K by complex eigenfrequencies and the equations for the forward and time-reversed wavefields are the same (Liu & Tromp 2008). Therefore, for a sufficiently long time record, where $\Delta\tau \gg \frac{1}{\Delta\omega}$, $\Im_{JK} \approx \frac{1}{2}\delta_{JK}\Delta\tau \cos\omega_K t$, and to first order

$$\begin{aligned}\mathbf{S}_M(t) &= \sum_J \frac{1}{\omega_J}|\mathbf{J_M}\rangle\langle\mathbf{J_R}| \sum_K \frac{1}{\omega_K}|\mathbf{K_R}\rangle\langle\mathbf{K_E}|\mathbf{F_E}\rangle\frac{1}{2}\delta_{JK}\Delta\tau\cos\omega_K t \\ &= \sum_K \frac{1}{\omega_K^2}|\mathbf{K_M}\rangle\langle\mathbf{K_R}|\mathbf{K_R}\rangle\langle\mathbf{K_E}|\mathbf{F_E}\rangle\frac{1}{2}\Delta\tau\cos\omega_K t. \end{aligned} \tag{11}$$

It is interesting to note some differences between the acoustic case and the elastic case. In the acoustic case (scalar case), the system of forces $\mathbf{F}_E$ is reduced to a scalar value F_E. The time reversal of acoustic waves by mode theory has been investigated in Draeger & Fink (1999). They obtained the remarkable cavity equation for acoustic waves when the observation point M is located at the source point E

$$G_{RE}(t) * F_E.G_{ER}(-t) = G_{RR}(t) * F_E.G_{EE}(-t) = \sum_K \frac{F_E}{{\omega_K}^2} u_K^2(R)\, u_K^2(E)\frac{1}{2}\Delta\tau\cos\omega_K t. \tag{12}$$

The Green's functions G_{EE} and G_{RR} are the backscattering impulse response at points R and E. So the time-reversal field $S_E(t)$ at point E is the convolution of these two backscattering impulse responses $G_{EE}(-t)$ by $G_{RR}(t)$. Acoustic experiments in a chaotic cavity (Draeger *et al.* 1999) demonstrate that it is very good approximation.

In the elastic case, the cavity equation is no longer valid. The equivalent of the cavity equation is more complex as demonstrated in Appendix B. It is now necessary to take account of the tensorial character of Green's functions and of the difference between bra and ket. If only the dominant diagonal elements of $\Im_{JK}(t)$ are taken into account,

$$\mathbf{G_{RE}}(t) * \mathbf{F_E}.\mathbf{G_{ER}}(-t) = \sum_K |\mathbf{K_E}\rangle\langle\mathbf{K_R}|\mathbf{K_R}\rangle\langle\mathbf{K_E}|\mathbf{F_E}\rangle\frac{\Im_{KK}}{\omega_K^2} \tag{13}$$

and

$$\mathbf{G_{RR}}(t) * \mathbf{F_E}.\mathbf{G_{EE}}(-\mathbf{t}) = \sum_K |\mathbf{K_R}\rangle\langle\mathbf{K_R}|\mathbf{K_E}\rangle\langle\mathbf{K_E}|\mathbf{F_E}\rangle\frac{\Im_{KK}}{\omega_K^2}. \tag{14}$$

So it is easily seen that generally $|\mathbf{K_R}\rangle\langle\mathbf{K_R}|\mathbf{K_E}\rangle\langle\mathbf{K_E}| \neq |\mathbf{K_E}\rangle\langle\mathbf{K_R}|\mathbf{K_R}\rangle\langle\mathbf{K_E}|$. Actually, the scalar product $\langle\mathbf{K_R}|\mathbf{K_R}\rangle$ appears in eq. (13) whereas the scalar product $\langle\mathbf{K_R}|\mathbf{K_E}\rangle$ is present in eq. (14). Therefore, we must be cautious when extending results from the scalar acoustic waves to the elastic case.

2.3 Degenerate modes in azimuthal number *m*

A particular case comes up when the eigenfunctions are degenerate, which is the case for a SNREI Earth model. In eq. (A3), $\sum_K$ (resp.$\sum_J$) can be written explicitly $\sum_K = \sum_k \sum_m$ (resp. $\sum_J = \sum_j \sum_{m'}$), with $k = \{n, \ell\}$ (resp.$j = \{n', \ell'\}$). The eigenvector is $|\mathbf{K_R}\rangle = {}_{\mathbf{n}}\mathbf{D}_\ell(r)Y_\ell^m(\theta,\phi)$ and the eigenfrequency only depend on n and ℓ. In the general case, the eq. (8) can be rewritten

$$\mathbf{S}_M(t) = \sum_{n',\ell',m'} {}_{\mathbf{n}'}\mathbf{D}_{\ell'}Y_{\ell'}^{m'}(\mathbf{r_M})Y_{\ell'}^{m'*}{}_{\mathbf{n}'}\mathbf{D}_{\ell'}^{\dagger}(\mathbf{r_R}) \sum_{n,\ell,m} {}_{\mathbf{n}}\mathbf{D}_\ell Y_\ell^m(\mathbf{r_R})Y_\ell^{m*}{}_{\mathbf{n}}\mathbf{D}_\ell^{\dagger}(\mathbf{r_E})F_E\frac{\Im_{jk}(t)}{{}_n\omega_{\ell n'}\omega_{\ell'}}. \tag{15}$$

Downloaded from http://gji.oxfordjournals.org/ at INIST-CNRS on October 28,

In a first step, for sake of simplicity, let us consider the vertical component of the displacement, by assuming that the force is also applied vertically and that only the radial (vertical) component is rebroadcast. In that case, $\mathbf{u}_K(r,\theta,\phi) = {}_nU_\ell(r)Y_\ell^m(\theta,\phi)\hat{\mathbf{e}}_\mathbf{r}$. Using two times the addition theorem (or closure relationship) for spherical harmonics (eq. A7)

$$S_M^r(t) = \sum_{n',\ell',m'} {}_{n'}U_{\ell'}Y_{\ell'}^{m'}(\mathbf{r_M})_{n'}U_{\ell'}Y_{\ell'}^{m'*}(\mathbf{r_R})\sum_{n,\ell,m}{}_nU_\ell Y_\ell^m(\mathbf{r_R})_nU_\ell Y_\ell^{m*}(\mathbf{r_E})F_E\frac{\Im_{jk}(t)}{{}_n\omega_{\ell n'}\omega_{\ell'}}$$
$$= \sum_{n',\ell'}{}_{n'}U_{\ell'}^M P_{\ell'}^0(\cos\Delta_{RM})_{n'}U_{\ell'}^R\sum_{n,\ell}{}_nU_\ell^R P_\ell^0(\cos\Delta_{ER})_nU_\ell^E F_E\frac{\Im_{jk}(t)}{{}_n\omega_{\ell n'}\omega_{\ell'}}. \quad (16)$$

The same kind of calculation on radial component was performed for different applications by Fukao *et al.* (2002) and Tanimoto (2008). According to Romanowicz (1987) and Romanowicz *et al.* (2008), it is possible to apply a stationary phase approximation by using an asymptotic expression of $Y_\ell^m(\theta,\phi)$: $Y_\ell^m(\theta,\phi) = \frac{1}{\pi\sqrt{\sin\theta}}\cos[(\ell+1/2)\theta + m\frac{\pi}{2} - \frac{\pi}{4}]e^{im\phi}$. For a source at the pole, θ plays the role of epicentral distance Δ_{ER}. It is possible to use the Watson's theorem (see e.g. Aki & Richards 1980)

$$\sum_{\ell=0}^{\infty} f(\ell+1/2) = \int_{-\infty}^{\infty} f(\nu)e^{-i\pi\nu}\sum_{q=0}^{\infty}e^{-2i\pi\nu q}d\nu.$$

Then, the sum on modes is replaced by a sum on trains (with index q). We get rid of the sum on index ℓ but not of the sum over n.

By replacing in the expression of $\mathbf{S}_M(t)$ the Legendre polynomials by their asymptotic form, the stationary phase theorem can be applied. The contribution of the product of Legendre polynomials $P_\ell^0(\cos\Delta_{RM}).P_\ell^0(\cos\Delta_{ER})$ to $\mathbf{S}_M(t)$ can then be estimated. The product $P_{\ell'}^0(\cos\Delta_{RM})P_\ell^0(\cos\Delta_{ER})$ is maximum (Romanowicz 1987) when points E, R and M are on the same great circle, which corresponds to $\gamma_{ER} - \gamma_{EM} = 0$ or π (see Fig. 1). The phase terms present in the different wavetrains of the asymptotic expressions, will be maximum when $\Delta_{RM} = \Delta_{ER} \pm n\pi$, therefore when point M is located at point E or its antipode. This point is perfectly illustrated by fig. 2 of Tanimoto (2008). Since the contributions of each eigenfrequency tend to cancel out, all sinusoids will be in phase and interfere constructively when $t = 0$. In conclusion, the contribution to the time-reversed displacement will be maximum when point M is at point E and at time $t = 0$.

There will be also some non null contributions to time-reversed seismograms for some stationary phases, corresponding to particular group velocities. In that case, some ghost wavetrains will appear as demonstrated by Capdeville *et al.* (2000) corresponding to the neglected interaction between singlets of the same multiplet and the coupling between different multiplets (see neglected terms of eq. 10). A simple way to get rid of these ghost trains consists in sending back as many seismograms as possible which will interfere destructively. It is interesting to note that in the degenerate case, the time-reversed field from one station is a succession of progressive wavetrains with no clear extremum, except at the hypocentre and the antipode of the station though not at a specific time.

For the three-components of displacement, the same kind of calculation can be performed, but the vectorial operators ${}_\mathbf{n}\mathbf{D}_\ell$ impose to use the more general addition theorem as defined by eq. (A8) (see e.g. Li & Tanimoto 1993; Capdeville *et al.* 2000), which introduces generalized Legendre functions $P_\ell^{NN'}(\cos\Delta)$ with $N\epsilon[-1,+1]$ for a force system and with $N\epsilon[-2,+2]$ for a moment tensor. For sake of simplicity, the notation of Woodhouse & Girnius (1982) can be used and eq. (11) can be rewritten

$$\mathbf{v}.\mathbf{S_M}(t) = \sum_{n',\ell'}\sum_{m'}\sum_{N'=-1}^{+1}\mathbf{R_{kN'}}(\mathbf{r_M})Y_{\ell'}^{N'm'}(\theta_M,\phi_M)Y_{\ell'}^{m'*}(\theta_R,\phi_R)_{\mathbf{n}'}\mathbf{D}_{\ell'}^\dagger(r_R)\sum_{n,\ell}\sum_m\sum_{N=-1}^{+1}{}_\mathbf{n}\mathbf{D}_\ell(r_R)Y_\ell^m(\theta_R,\phi_R)\mathbf{Q_{kN}}(\mathbf{r_E})Y_\ell^{N'm*}(\theta_E,\phi_E)\frac{\Im_{jk}(t)}{{}_n\omega_{\ell n'}\omega_{\ell'}}, \quad (17)$$

where $\mathbf{v}$ is the instrumental response. The source term $\mathbf{Q_{kN}}(\mathbf{r_E})Y_\ell^{Nm*}(\theta_E,\phi_E)$ can be found from $\langle\mathbf{u_K}|\mathbf{F}\rangle(r_E,\theta_E,\phi_E) = \sum_{N=-1}^{N=1}Q_{kN}(r_E)Y_\ell^{Nm*}(\theta_E,\phi_E)$. It is replaced by $\mathbf{S_{kN}}(\mathbf{r_E})Y_\ell^{Nm*}(\theta_E,\phi_E)$ if the source force is the gradient of the moment tensor $\mathbf{M}$. $\mathbf{R_{kN}}(\mathbf{r_M})$, $\mathbf{S_{kN}}(\mathbf{r_M})$ are detailed in Woodhouse & Girnius (1982). Similarly to a point force, the same formula applies for $\mathbf{S_{kN}}$ (for a moment tensor). It is again possible to use two times the generalized addition theorem (eq. A8). After some calculations, an expression similar to eq. (16) is obtained, but the simple Legendre polynomials $P_\ell^0(\cos\Delta)$ are replaced by $P_\ell^{NN'}(\cos\Delta)$ with the appropriate phase effects. By applying the same stationary phase approximations and expansions of the generalized spherical harmonics (see e.g. Capdeville *et al.* 2000), we end up with the same conclusions that the time-reversed signal is maximum when point M is located at the source point E at time $t = 0$.

3 FROM A THREE-POINT PROBLEM TO A MULTIPLE POINT-PROBLEM

In this section, we generalize eq. (11) to the case of many receivers (or many sources) in order to provide the basis for global seismology applications.

3.1 Time-reversal imaging: one source, *n* receivers

Let us consider that the Earth is covered by a global seismic network at points $\mathbf{r_{R_i}}, i = (1, n_R)$. Due to the fact that the Earth is covered by two-thirds of oceans and that most broadband seismic stations are installed in the northern hemisphere, the spatial coverage is obviously uneven. How much will the non-uniform spatial coverage of the Earth affect the destructive and constructive interferences which control the quality of the time-reversal focus? The ideal time-reversal mirror would be a perfectly uniform seismic network covering the whole surface of the Earth, much like the transducer arrays used in acoustics (Fink 1997, 2006). Since according to eqs (8) and (11), contributions of all

Downloaded from http://gji.oxfordjournals.org/ at INIST-CNRS on October 28, 2016

stations add linearly, a simple way to solve this problem consists in weighting each station by a surface s_i such that $\sum_{i=1}^{n_R} s_i = S_{\text{earth}}$, S_{earth} being the surface of the Earth. The time-reversed field at any point M at the surface of the Earth is then

$$\mathbf{S'_M}(t) = \sum_{i=1}^{n_r} s_i S^i_M(t) = \sum_{i=1}^{n_r} s_i \sum_K \sum_J \frac{1}{\omega_K \omega_J} |\mathbf{J_M}\rangle \langle \mathbf{J^i_R} | \mathbf{K^i_R}\rangle \langle \mathbf{K_E} | \mathbf{F_E}\rangle \, \Im_{JK}(t). \tag{18}$$

If the spatial coverage by receivers is dense enough, the sum $\sum_i s_i$ can be replaced by the surface integral $\int_{\text{earth}} dS$. The eigenfunctions $|\mathbf{K_R}\rangle$, $|\mathbf{J_R}\rangle$ at receiver stations are considered at the surface of the Earth $r_R = R_{\text{earth}}$. In the degenerate case, according to (Woodhouse & Girnius 1982, see Appendix A),

$$|\mathbf{K_R}\rangle = {}_{\mathbf{n}}\mathbf{D}_\ell(r_R) Y^m_\ell(\theta, \phi) = \sum_{N=-1}^{N=1} D^N_k(r_R) Y^{Nm}_\ell(\theta_R, \phi_R) \hat{\mathbf{e}}^N$$

with $\hat{\mathbf{e}}^N$ is one vector of the generalized complex-value basis $\{\hat{\mathbf{e}}^-, \hat{\mathbf{e}}^{\mathbf{0}}, \hat{\mathbf{e}}^+\}$.

Now, we can integrate over the whole surface of the Earth Σ_{earth}:

$$\sum_{i=1}^{n_R} s_i \langle \mathbf{J^i_R} | \mathbf{K^i_R}\rangle = \int_{\text{earth}} dS \left(\sum_{N=-1}^{N=1} D^{N\dagger}_k(r_R) Y^{Nm*}_\ell(\theta, \phi) \right) \left(\sum_{N'=-1}^{N'=1} D^{N'}_{k'}(r_R) Y^{N'm'}_{\ell'}(\theta, \phi) \right) \hat{\mathbf{e}}^N \hat{\mathbf{e}}^{N'}. \tag{19}$$

Finally, by using the orthogonality of the basis vectors $\hat{\mathbf{e}}^N$, the orthonormality of generalized spherical harmonics (eq. A4) and eigenvectors (eq. A5), for $M = E$, we obtain

$$\mathbf{S'_E}(t) = \sum_k |\mathbf{K_E}\rangle \langle \mathbf{K_E} | \mathbf{F_E}\rangle {D_k}^2(r_R) \frac{\Delta\tau \cos \omega_k t}{2\omega_k^2}, \tag{20}$$

where ${D_k}^2(r_R)$ is defined in Appendix A (eq. A5). This expression is maximum for $t = 0$ since it is the only time where all cosine terms add constructively.

An alternative but equivalent demonstration can be done by starting from eq. (18) by using the generalized addition theorem of eq. (A8), with the point E at the pole.

At any point M at the surface of the Earth, the calculation done in Section 2.1 is still valid, except that the eigenfunctions in point $\mathbf{r}_M$ must be introduced. The surface scalar product of eq. (19) is readily calculated (see eq. A3)

$$\mathbf{S'}(\mathbf{r}_M, t) = \sum_k |\mathbf{K_M}\rangle \langle \mathbf{K_E} | \mathbf{F}(\mathbf{r_E})\rangle D^2_k(r_R) \frac{1}{2\omega_k^2} \Delta\tau \cos \omega_k t. \tag{21}$$

The time derivative of this expression looks like the Green's function as defined in eq. (A14) except that the force system $|\mathbf{F}(\mathbf{r}_{\text{E}})\rangle$ is weighted by the duration of the time-reversed seismogram $\Delta\tau$ and an eigenfunction dependent term $D^2_k(r_R)$. In the degenerate Earth, all contributions from the different modes will tend, in average, to cancel out, except for time $t = 0$ and when the point $M = E$. Therefore, for $t = 0$ and for the acceleration of $\mathbf{S}(\mathbf{r}_{\text{M}}, t)$, it is found that the maximum of the time-reversed signal is proportional to the force system $\mathbf{F}(\mathbf{r_E})$, but it is weighted by the eigenfunctions at the surface of the Earth.

3.2 Cross-correlations: *n* sources, two receivers

Due to spatial reciprocity, using n receivers at $\mathbf{r_R}$ as a Time Reversal Mirror is equivalent to stacking the cross-correlations of the signal recorded in E and M produced by each source placed at $\mathbf{r_R}$. Due to the linearity of the problem, the latter is also the same as doing the cross-correlation of the signal recorded in R and M produced by the n sources simultaneously, as it is the case of signal due to the distribution of random noise sources (Derode *et al.* 2003). Actually, there are two ways for investigating the effect of a random distribution of seismic sources, either, by considering scattered waves in a multiply scattering medium, or by stacking a random distribution of sources through time in any kind of elastic medium.

3.2.1 One seismic noise source

In this section, we explore the convergence of the cross-correlation of seismic signals recorded at two points R and M to the Green's function between R and M for one seismic source. The two Green's functions $G_{ER}(t)$ and $G_{EM}(t)$ are given by eq. (A14) and the corresponding seismograms of displacement due to a point force system $\mathbf{F_E}$ are

$$\begin{cases} \mathbf{u_R}(t) = \mathbf{F_E}.\mathbf{G_{ER}}(t) = \sum_K |\mathbf{K_R}\rangle \langle \mathbf{K_E} | \mathbf{F_E}\rangle H(t) \dfrac{\sin \omega_K t}{\omega_K} \\ \mathbf{u_M}(t) = \mathbf{F_E}.\mathbf{G_{EM}}(t) = \sum_J |\mathbf{J_M}\rangle \langle \mathbf{J_E} | \mathbf{F_E}\rangle H(t) \dfrac{\sin \omega_J t}{\omega_J} \end{cases} \tag{22}$$

The cross-correlation CC of $\mathbf{G_{ER}}(t) \otimes \mathbf{G_{EM}}(t)$ involves the same integral $\Im_{JK}(t)$ as in eq. (8)

$$CC(\tau) = \int_{t_1}^{t_2} \mathbf{u_R}(t) \mathbf{u^\dagger_M}(t + \tau) \, dt = \sum_K \sum_J |\mathbf{K_R}\rangle \langle \mathbf{F_E} | \mathbf{K_E}\rangle \langle \mathbf{J_E} | \mathbf{F_E}\rangle \langle \mathbf{J_M}| \frac{\Im_{JK}(\tau)}{\omega_J \omega_K}. \tag{23}$$

Downloaded from http://gji.oxfordjournals.org/ at INIST-CNRS on October 28

The expression in eq. (23) has many similarities with eq. (11) but shows some differences. The role of point R is played by point E. More importantly, we now have to handle a 2×2 tensor $CC(\tau)$, (due to the double inner product $\langle \mathbf{F}_\mathrm{E}|\mathbf{K}_\mathrm{E}\rangle\langle \mathbf{J}_\mathrm{E}|\mathbf{F}_\mathrm{E}\rangle$) instead of a vector $\mathbf{S_M}(t)$ with only one inner product $\langle \mathbf{K}_\mathrm{E}|\mathbf{F}_\mathrm{E}\rangle$. In the case of non-degenerate elastic modes, and if we assume that the seismic wavefields $\mathbf{u_R}(t)$ and $\mathbf{u_M}(t)$ are diffuse, there is equipartition of energy between modes, meaning that the modal amplitudes are uncorrelated random variables (Lobkis & Weaver 2001): the average of excitation coefficients $\langle \mathbf{K}_\mathrm{E}|\mathbf{F}_\mathrm{E}\rangle\langle \mathbf{J}_\mathrm{E}|\mathbf{F}_\mathrm{E}\rangle$ is proportional to $\delta_{JK} F_E^2$. This point was also carefully addressed by Tsai (2010). Eq. (23) shows that the time derivative of $CC(\tau)$ is equal to $\sum_K |\mathbf{K_R}\rangle\langle \mathbf{K_M}| \frac{-F_E^2 \Delta\tau \sin\omega_K t}{2\omega_K}$ and therefore proportional to the Green's function (eq. A14) weighted by the spectral energy density and $\Delta\tau = t_2 - t_1$. In our calculations based on TRM, we only consider positive times t_1 and t_2. But for cross-correlation applications, it is possible to consider negative time t_1, to retrieve $G_{RM}(t) - G_{RM}(-t)$. If sources are only located at the surface of the Earth, the equipartioning of energy is usually not fulfilled and the backscattering response has to be removed (i.e. deconvolved) from the cross-correlation (Derode *et al.* 2003). It has to be noted that the Green's function is simply retrieved in case of diffuse fields as demonstrated by Campillo & Paul (2003) because the recorded signal has no longer dependence on the original point. As discussed by Snieder (2004), the equipartitioning of energy is far from perfect since the time is too short for the Earth normal modes to equilibrate, but the global requirement of equipartitioning of normal modes can be relaxed to the local requirement of isotropic coverage of the incident angle of incoming waves at the receivers.

In the case of degenerate elastic modes (which is the case for the Earth normal modes at long-period in a SNREI reference model), we can apply twice the generalized addition theorem and an expression similar to eq. (17) is found implying $P_\ell^{NN'}(\cos\Delta_{ME})$ and $P_\ell^{NN'}(\cos\Delta_{RE})$.

$$\mathbf{S_M}(t) = \sum_{n',\ell'} \sum_{N'=-1}^{+1} {}_{\mathbf{n}'}\mathbf{D}_\ell^{\mathbf{N}'}(\mathbf{r_R}) \sum_{m'} Y_{\ell'}^{N'm'}(\theta_R,\phi_R) Y_{\ell'}^{N'm'*}(\theta_E,\phi_E)\, {}_{\mathbf{n}'}\mathbf{D}_{\ell'}^{\mathbf{N}'\dagger}(\mathbf{r_E})\mathbf{F}(\mathbf{r_E})$$
$$\times \sum_{n,\ell} \sum_{N=-1}^{+1} \mathbf{F}^\dagger(\mathbf{r_E})_{\mathbf{n}}\mathbf{D}_\ell^{\mathbf{N}}(\mathbf{r_E}) \sum_m Y_\ell^{Nm}(\theta_E,\phi_E) Y_\ell^{Nm*}(\theta_M,\phi_M)\, {}_{\mathbf{n}}\mathbf{D}_\ell^{\mathbf{N}\dagger}(\mathbf{r_M}) \frac{\Im_{jk}(t)}{{}_n\omega_{\ell n'}\omega_{\ell'}} \tag{24}$$

By using the same arguments as in Section 2.2.3 (stationary phase approximation), it can be demonstrated that the most important contributions to $CC(\tau)$ are provided by sources located along the great-circle aligned with points R and M.

3.2.2 Random distribution of seismic noise sources

Another way to approach to the Green's function by cross-correlation technique consists in considering a random distribution of noise sources (Shapiro *et al.* 2005). For a homogeneous random distribution of seismic noise sources, the same kind of calculation as in Section 3.1 can be performed as well. Let us first consider a homogeneous 3-D distribution of sources F_E with a density distribution $n(r,\theta,\phi)$ in the whole Earth. Each source can be associated with a volume $a_n(r,\theta,\phi)$ such that, if only the case $J = K$ is considered, we can replace in eq. (23) the sum on the contributions of all sources by a volume integral

$$\sum_n a_n(r,\theta,\phi)\langle \mathbf{F_E}|\mathbf{K_E}\rangle\langle \mathbf{K_E}|\mathbf{F_E}\rangle = \int_V n(r,\theta,\phi)\mathbf{F_E^\dagger}\mathbf{u_K}(\mathbf{r_E})\mathbf{u_K^\dagger}(\mathbf{r_E})\mathbf{F_E}\, dV.$$

If all sources are considered as identical and uniformly distributed in the volume, it is only necessary to calculate the integral $\int_V \mathbf{u_K}(\mathbf{r_E})\mathbf{u_K^\dagger}(\mathbf{r_E})\, dV$ which is equal to the identity operator. Then eq. (23) reduces to

$$CC(\tau) = \langle \mathbf{F_E}|\mathbf{F_E}\rangle \sum_K |\mathbf{K_R}\rangle\langle \mathbf{K_M}| \frac{\Im_{kk}(\tau)}{\omega_k^2}. \tag{25}$$

When taking a force system with a norm equal to 1, the time derivative of CC is the Green's function (multiplied by $\Delta\tau$). So, we perfectly understand why it is usual to whiten spectral density or to binarize the seismograms such as in Derode *et al.* (1999) to homogenize the contributions of all noise sources. This result is identical to the case of equipartitioning of modal energy (Lobkis & Weaver 2001; Tsai 2010), but the role of multiple scatterers of a diffusive medium is played by the stack of uniformly identical distributed noise sources.

However, most seismic noise sources are due to the interaction between solid and fluid Earth (e.g. Rhie & Romanowicz 2004). They are primarily located at the surface of the Earth. With a density distribution $n(\theta,\phi)$ of identical sources associated with a surface $s_i(\theta,\phi)$ normalized such that $\int_S n(\theta,\phi)\sin\theta\, d\theta\, d\phi = 1$, and if the case $J = K$ is considered, then it is possible to integrate

$$CC(\tau) = \sum_K |\mathbf{K_R}\rangle\langle \mathbf{K_M}| \left[\sum_{\gamma\zeta} {F_E}^{\dagger\gamma} \int_S n(\theta,\phi)\, \sin\theta\, d\theta\, d\phi\, |\mathbf{K_E^\gamma}\rangle\langle \mathbf{K_E^\zeta}|{F_E}^\zeta \right] \frac{\Im_{kk}(\tau)}{\omega_k^2}. \tag{26}$$

We keep the possibility for having different forces on the vertical and the horizontal components. By using orthonormalization of eigenfunctions, according to eq. (A5), and the addition theorem for $J = K$ (eq. A4), it is possible to calculate the nine components of cross-correlation tensor CC

$$CC_{\beta\alpha}(\tau) = \sum_K |\mathbf{K_R^\beta}\rangle\langle \mathbf{K_M^\alpha}| \sum_\gamma F_E^{\gamma 2} D_k^{\gamma 2}(r_E) \frac{\Im_{kk}(\tau)}{\omega_k^2}. \tag{27}$$

Downloaded from http://gji.oxfordjournals.org/ at INIST-CNRS on October 28, 2016

The time derivative of *CC* is proportional to the Green's function (tensor in the elastic case) of velocity between points *M* and *R* (see eq. A15). This equation has many similarities with the Green's tensor $G_{RM}(t)$ between M and R. But it is not the Green's tensor since the proportionality factor is frequency dependent. It is weighted by the square of amplitude of sources at the Earth surface (as noted by Tanimoto 2008, for a vertical force), and of the eigenfunctions which must be taken at the surface of the Earth. That explains why the signal obtained by *CC* is basically dominated by the fundamental modes since microseisms are generated by the oceanic effects which only act on the Earth's surface. The bias[2] in seismic interferometry related to the 2-D- instead of 3-D-source distribution has been carefully investigated by Halliday & Curtis (2008) and Kimman & Trampert (2010). They show that when sources are located at the surface of the Earth, the recovery of surface wave higher modes can be problematic. For getting the real Green's tensor, the distribution of noise sources should be distributed within the whole 3-D volume and not only at the surface of the Earth. Another basic difference between TRM and CCT is the fact that CCT is related to the square of the amplitude of the force system, whereas, for TRM, the reversed vector field is linearly related to the force system $\mathbf{F_E}$.

These calculations show, through normal mode theory, how the time-reversal (adjoint field) approach, and cross-correlations of seismograms are related (see Derode *et al.* 2003, for the acoustic case) and that the same kind of calculations apply in both cases for acoustic and elastic waves.

4 DISCUSSION AND APPLICATIONS

We develop in previous sections the whole theory of TR method by using the normal mode formalism. This theory was already implemented in Larmat *et al.* (2006) for the Sumatra-Andaman mega-earthquake on 2004 December 26. It is only valid at very long periods (>100 s) when the degenerate normal modes of SNREI model provide a correct Green's function. The normal mode theory enables us to separate the radial and lateral variations of physical parameters and to clearly show the limitations of TRM and cross-correlation techniques. At shorter periods (<100 s), it is necessary to use purely numerical techniques such as spectral element method to incorporate 3-D Earth models for computing a more accurate Green's function, such as done by Larmat *et al.* (2008). An important result is that the focusing at the epicentre is largely dependent on the weighting of stations as defined in Section 3.1, eventhough the TRM is very robust since it is based on the constructive or destructive interference of waves primarily dependent upon the phase information. If the contribution of the different stations is not correctly taken into account, the focus point may still be correctly located in time and space, but the information on amplitude, that is, on the radiation pattern will be lost. This weighting is particularly important when the station distribution is non-uniform, which is the case of the current instrument global coverage. Most broad-band stations are located in continents and primarily in the northern hemisphere.

4.1 Voronoi cells

A simple way to take account of the uneven distribution is to use a Voronoi tessellation. This kind of mapping at the surface of the Earth was implemented, for example, for global tomography by Debayle & Sambridge (2004) and for time-reversal earthquake location by Larmat *et al.* (2006). An example of Voronoi cell distribution is shown in Fig. 3 for a global distribution of 115 stations. As it can be seen, the surface distribution is very heterogeneous and some stations in the Pacific, Atlantic and Indian oceans may have a very large contribution associated with large cells because of their isolation degree. Other stations in north America, Europe and eastern Asia have a very small contribution with minute cells. Fig. 4 shows a synthetic example of focusing of time-reversed seismograms (an example of seismogram is given on Fig. 4a) for an isotropic source located close to Sumatra obtained by using the 115 stations of Fig. 3 weighted by the Voronoi cells area. Fig. 4(b) shows a perfect refocusing when using the Voronoi cell tessellation. It was implemented on a routine basis for locating tectonic earthquakes by Larmat *et al.* (2006) and glacial earthquakes by Larmat *et al.* (2008). When the spatial and the azimuthal coverage around the seismic source is very poor, the radiation pattern at the origin time is not correctly recovered as will be discussed in Section 4.4 (see Fig. 5).

4.2 One-bit discretization

In calculations of Section 2, we have used arguments based on the stationary phase approximation, emphasizing the importance of the phase information for building the focusing of time-reversed wavefield. Fig. 4(c) shows binarized seismograms which suppress the information on the amplitude of seismograms. Binarization of seismograms is routinely used when calculating empirical Green's functions by cross-correlation between two stations (Shapiro *et al.* 2005). When binarized seismograms are time-reversed with the appropriate weighting scheme, the focusing is almost as good as the focusing obtained by time-reversal of complete seismograms but not the radiation pattern of the explosion (Fig. 4d). This experiment demonstrates that the information is primarily conveyed by the phase of seismograms. It is not really a surprise, since the location of the earthquake and the focusing time correspond to a constructive interference of the whole parts of seismograms.

4.3 Method for inverting a force system

According to eq. (20), it is possible to obtain a linear system of equations which enables us to retrieve the vector force $\mathbf{F_E}$. This method might be automatized on a routine basis to retrieve the force system. We only recall the results developed in Section 3.1. The different Green's

[2] Correction added after online publication 2012 September 6: the word 'bins' has been corrected to 'bias'.

Downloaded from http://gji.oxfordjournals.org/ at INIST-CNRS on October 28

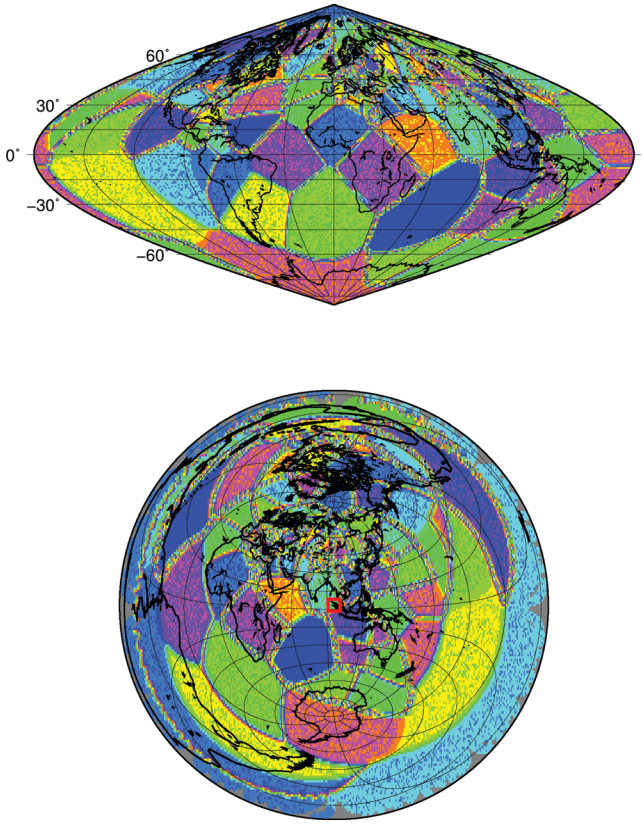


Figure 3. Voronoi cells used for time-reversal of Sumatra-Andaman earthquake for a global network of 115 stations. Each cell is associated with a station. The area of each cell reflects the global coverage of the Earth by seismic networks.

function components between points $\mathbf{r_E}$ and $\mathbf{r_R}$ are equal to

$$G_{\beta\gamma}(\mathbf{r_E}, \mathbf{r_R}, t) = \sum_K |\mathbf{K_R^\beta}\rangle\langle\mathbf{K_E^\gamma}| \frac{H(t)\ \sin\omega_k t}{\omega_k}$$

and the corresponding displacement components are $u_R^\beta(\omega) = \sum_K \sum_\gamma |\mathbf{K_R^\beta}\rangle\langle\mathbf{K_E^\gamma}|\mathbf{F_E^\gamma}\rangle \frac{H(t)\sin(\omega_K t)}{\omega_K}$. For a uniform distribution of stations R_i at the surface of the Earth, the contribution of stations is weighted by using, for example, a Voronoi tessellation (Fig. 3). At point source $\mathbf{r_E}$, the eq. (20) by reordering the different terms, can be written for each component of displacement

$$\mathbf{S}_E^\alpha(t) = \sum_\gamma \left[\sum_{n\ell} {}_nD_\ell^\alpha(r_E)\, {}_nD_\ell^2(0)\, {}_nD_\ell^{\gamma *}(r_E) \frac{\Im_{kk}(t)}{\omega_k^2} \right] F_E^\gamma = \sum_\gamma P_{\alpha\gamma} F_E^\gamma. \tag{28}$$

All oscillations are in phase for $t = 0$ [$\Im_{kk}(0) = 0.5\Delta\tau$], which explains why focusing of energy is obtained at that time. We then obtain a matrix relationship $\mathbf{S}(t{=}0) = \mathbf{PF_E}$ and the force system $\mathbf{F}_\mathrm{E}$ can be retrieved by inversion of the matrix $\mathbf{P}$. This linear system with respect to the different components $\mathbf{F_E}$, is particularly simple and can be easily inverted and implemented.

From a practical point of view, it is first necessary to locate the source by TR method in time and space, finding where the amplitude is maximum. The three components of $S_E(t_0)$ can be stored. Once the initial source origin time t_0 and the corresponding location (r_E, θ_E, ϕ_E) are determined, it is possible to numerically calculate the different coefficients of the matrix $\mathbf{P}$ by normal mode summation through an iterative procedure. Synthetic seismograms at all receivers used in TRM can be computed for three delta functions at the focusing point. A new time-reversal inversion of these synthetic seismograms can then be performed and provide the amplitude at the focal point of the different elements of matrix $\mathbf{P}$. $\mathbf{P}$ can be seen as the TRM transfer function of the seismic network (or antenna) considered as a single instrument. By inverting the 3×3 matrix $\mathbf{P}$, the components of the force system $\mathbf{F_E}$ can be retrieved. An interesting application of this simple inversion technique might be the investigation of glacial earthquakes to make more quantitative the results of Larmat *et al.* (2008).

4.4 Time reversal of deformation—moment tensor inversion method

At the focusing point, and at time $t = 0$, the amplitude distribution reflects the surface wave radiation pattern of the event. Therefore, we can expect to get quantitative information on the seismic moment tensor associated with the earthquake. Fig. 5 shows that for tectonic earthquakes with different focal mechanisms (thrust and strike-slip events), the radiation pattern of the event at the epicentre is correctly retrieved provided that the station distribution and particularly, its azimuthal coverage around the source are uniform. This figure also demonstrates the

Downloaded from http://gji.oxfordjournals.org/ at INIST-CNRS on October 28, 2016

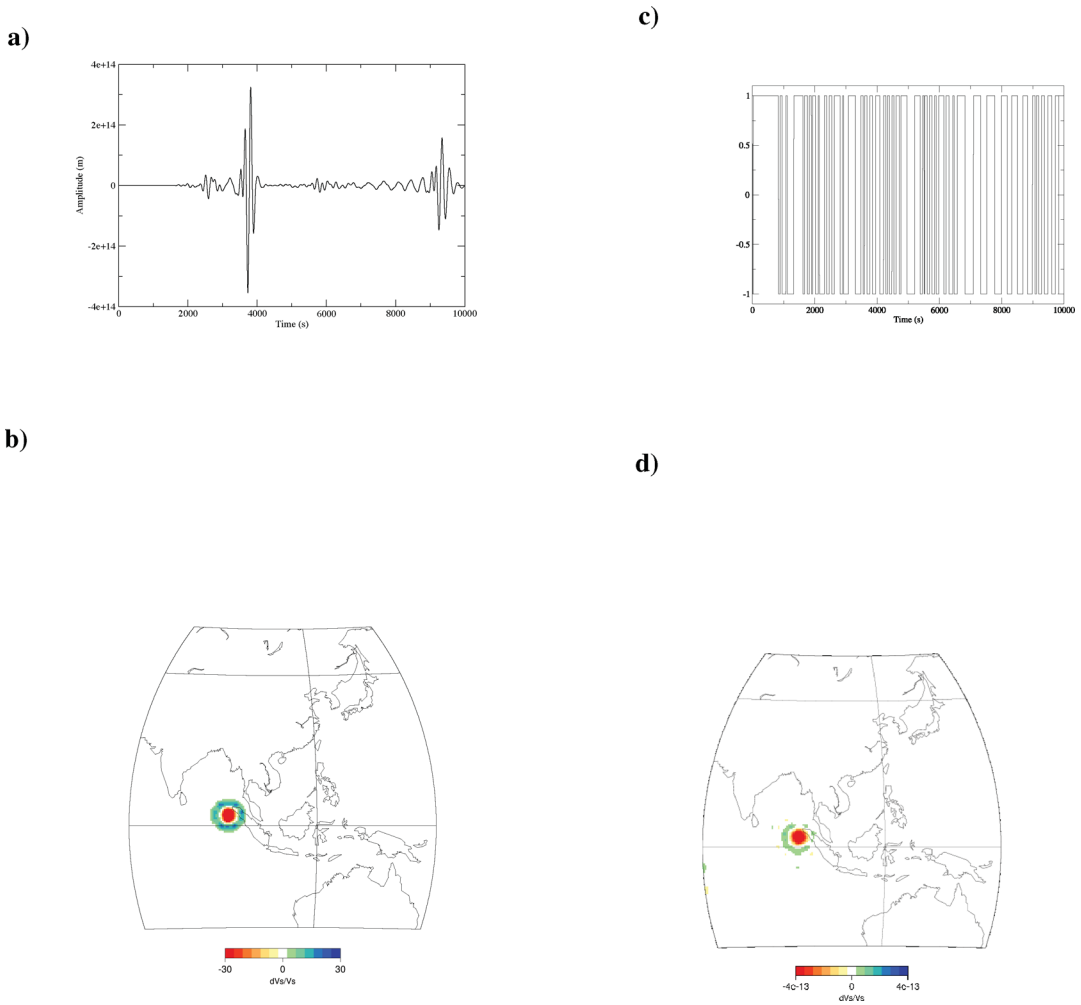


Figure 4. Synthetic example of focusing by the time-reversal method for an isotropic source for complete and one-bit seismograms (one-bit normalization versus amplitude time-reversal experiment). (a) Example of full seismogram calculated by normal mode summation. (b) Focusing of the complete seismic wavefield when weighting of stations by Voronoi tessellation (same distribution of stations as in Fig. 3). (c) Example of one-bit seismogram. (d) Focusing of one-bit discretized seismograms. The weighting of stations by Voronoi tessellation is applied.

complementarity and the differences between TRM and back-projection techniques (Ishii *et al.* 2005). When using an antenna such as US array, the radiation pattern around the source is lost by back-projection due to the limited array aperture, whereas TRM applied at the global scale provides the correct radiation pattern. TRM is primarily useful at very long periods ($T > 100$ s) and back-projection techniques using the first arrivals of body waves can be used at short periods and enable us to accurately retrieve the source time function.

To go further in the inversion of moment tensor, it is necessary to consider the deformation tensor. Following eq. (A16), the deformation operator $E = \frac{1}{2}(\nabla + \nabla^{\mathrm{T}})$ and the seismic moment tensor M can be introduced (see Appendix A). For a tectonic earthquake, it is usual to consider that the source time function is a Heaviside function, $H(t)$. By discarding the static term

$$\mathbf{u_R}(t) = -\sum_K |\mathbf{K_R}\rangle\langle\mathbf{K_E}\mathbf{E}|\mathbf{M}\rangle H(t)\frac{\cos\omega_K t}{\omega_K^2}. \tag{29}$$

For $t > 0$, the time derivative of $\mathbf{u_R}(t)$ has the same expression as for the source force system of eq. (A13). Therefore, it is possible to work with velocity seismograms instead of displacement seismograms for keeping the same theory. It is now necessary to calculate all components of the spatial derivatives of the Green's function at the source point $\mathbf{r_E}$ according to eq. (A16), such that

$$G_{\beta\gamma,\zeta}(\mathbf{r_E}, \mathbf{r_R}, t) = -\sum_K |\mathbf{K_R^\beta}\rangle\epsilon_{\gamma\zeta}^{K\star}(\mathbf{r_E})H(t)\frac{\cos\omega_k t}{\omega_k^2},$$

where the deformation tensor components are given by $\epsilon_K^{\gamma\zeta}(\mathbf{r_E}) = \frac{1}{2}\left(\frac{\partial|\mathbf{K_E^\gamma}\rangle}{\partial\xi_\zeta} + \frac{\partial|\mathbf{K_E^\zeta}\rangle}{\partial\xi_\gamma}\right)$. In a synthetic way, we can define the Green's tensor of the moment tensor by $\mathbf{G'_{ER}}(t) = \sum_K |\mathbf{K_E}\rangle\langle\mathbf{K_R}\mathbf{E}|\Im'_k(t)$, where $\langle\mathbf{K_R}\mathbf{E}|$ (respectively $|\mathbf{M}\rangle$) is either a 3×3 tensor or a 1×6 vector (resp. 6×1 vector).

The retrieval of the moment tensor is more difficult than the force system since the moment tensor M has six independent components. At this stage, two different approaches can be followed. We can either start from eq. (28) and replace $\langle\mathbf{K_E}|\mathbf{F_E}\rangle$ by $\langle\mathbf{K_E}\mathbf{E}|\mathbf{M}\rangle$ or we can calculate

Downloaded from http://gji.oxfordjournals.org/ at INIST-CNRS on October 28

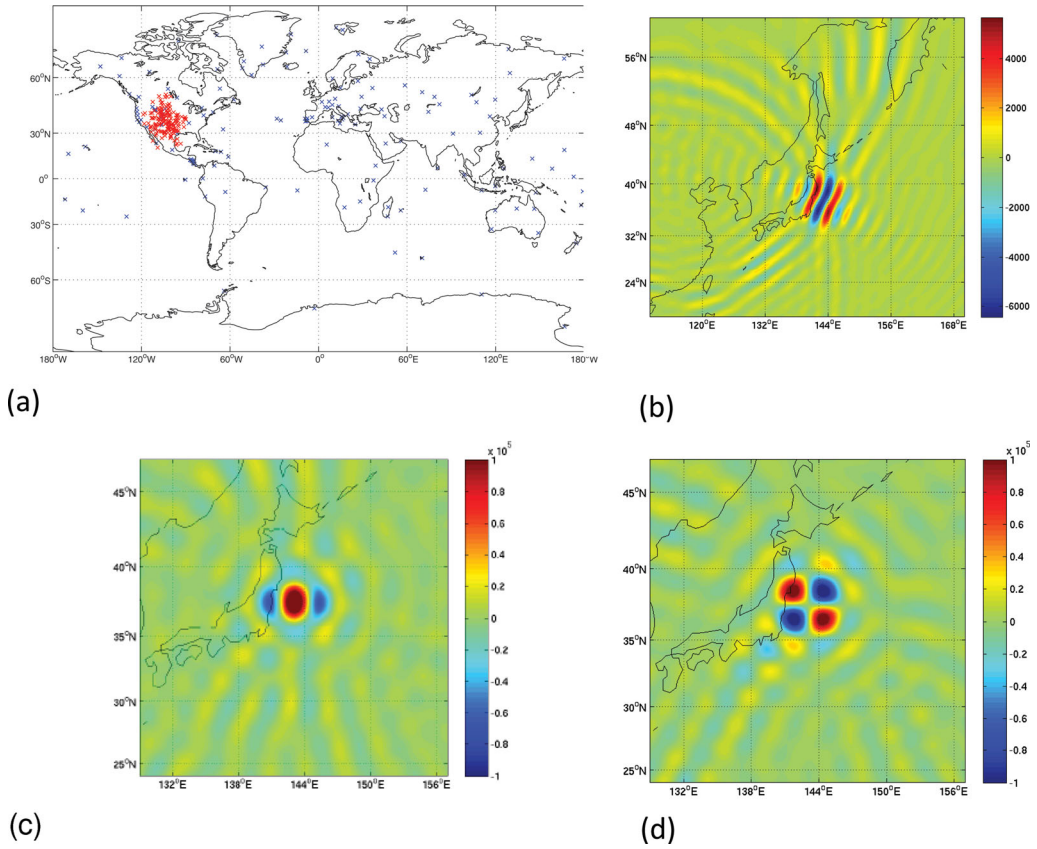


Figure 5. Sensitivity of the time-reversed field to the station distribution and the focal mechanism. (a) blue crosses: stations of the global network of F.D.S.N. (Federation of Digital Seismograph Network); red crosses: stations of an antenna of 180 stations in USA. Synthetic seismograms are calculated by normal mode summation, for a strike-slip fault in subparts (b) and (d), and for a reverse fault in subpart (c) located in eastern Japan. (b) TRM focusing obtained by using the USA antenna seismograms. (c) and (d) TRM focusing obtained for the global network seismograms.

the deformation field associated with the time reversed $\mathbf{S}'_{\mathbf{M}}(t)$,

$$\Xi(r_M, t) = \mathbf{G}'^{\dagger}_{RM}(t) * \mathbf{G}'_{ER}(-t) * \mathbf{M}(-t), \tag{30}$$

where G'_{ER} and G'_{RM} are the spatial derivatives associated with Green's functions G_{ER} and G_{RM}. At point source location E, the deformation field $\Xi_E(t)$ is given by

$$\Xi_E(t) = \sum_J |\mathbf{E}\mathbf{J}_{\mathbf{E}}\rangle\langle\mathbf{J}_{\mathbf{R}}|\mathbf{u}_{\mathbf{R}}(\mathbf{t}) = \sum_J \sum_K |\mathbf{E}\mathbf{J}_{\mathbf{E}}\rangle\langle\mathbf{J}_{\mathbf{R}}|\mathbf{K}_{\mathbf{R}}\rangle\langle\mathbf{K}_{\mathbf{E}}\mathbf{E}|\mathbf{M}\rangle\Im'_{JK}(t). \tag{31}$$

In the first case, we obtain a vector field (with three components) which will not enable us to retrieve the six components of the moment tensor but only the seismic radiation pattern (see Fig. 5). For the second approach, as proposed by Kawakatsu & Montagner (2008) and similar to the adjoint centroid-moment tensor inversion of Kim *et al.* (2011), the deformation tensor is calculated.

At this stage, if we have a homogenous distribution of stations, we can integrate over the whole network of stations $\langle\mathbf{J}_{\mathrm{R}}|\mathbf{K}_{\mathrm{R}}\rangle$ as done in Section 3.1. In a second step, the generalized addition theorem can be applied to $|\mathbf{E}\mathbf{K}_{\mathrm{E}}\rangle\langle\mathbf{K}_{\mathrm{E}}\mathbf{E}|$, and by using the orthonormalization of eigenfunctions and particularly of generalized spherical harmonics in the degenerate case, we can get a 6x6 matrix relating the six components of the time-reversed deformation field at the source $\Xi_E(t)$ to the six components of the moment tensor M. To ensure the symmetry of the calculation (Kawakatsu & Montagner 2008) such that $\Xi_E^{\alpha\zeta} = \Xi_E^{\zeta\alpha}$, we have to consider not only $G_{\beta\gamma,\zeta}$ but also $G_{\zeta\beta,\gamma}$, since the contribution of $M_{\zeta\gamma}$ must be the same as the contribution of $M_{\gamma\zeta}$. As in eq. (28), it is found a linear system with respect to the moment tensor components $\Xi_{\mathrm{E}}(0) = \mathbf{P}'\mathbf{M}$ at point E and for time $t = 0$. This simple approach will be developed and implemented in a future paper. Classical inversion techniques are based on the comparison between synthetic and real seismograms in the different stations, whereas TRM focus the whole broad-band information at the source location.

5 CONCLUSIONS

It is shown in this paper how the TRM, first developed in acoustics (Fink 1996) can be applied in global seismology. By using normal mode theory, it is demonstrated why and how TRM will enable seismic waves to focus and to give a maximum of signal at the right time and the right location of the seismic source. The similarities and differences with the cross-correlation technique have also been investigated.

Downloaded from http://gji.oxfordjournals.org/ at INIST-CNRS on October 28, 2016

From a practical point of view, the TRM is very easy to implement, and the location of seismic events does not need any assumption on a preliminary determination. In addition, provided that the synthetic Green's function of the Earth is accurate enough, TRM takes advantage of the whole broad-band frequency range of seismograms. Recently, the advances in numerical methods enable accurate simulations of seismic wave propagation (Komatitsch & Vilotte 1998; Komatitsch *et al.* 2002) in 3-D heterogeneous Earth models. Unfortunately, the main limitation is still the computing time. Normal mode eigenfunctions and eigenfrequencies can be computed very efficiently, and provide accurate Green's functions at periods longer than 100 s. Therefore, TRM using nomal mode theory can provide first and rapid locations in time and space of large earthquakes for global monitoring (Larmat *et al.* 2006) by focusing the complete broad-band information in a single point or a limited area for finite extent sources. Due to its inherent simplicity of implementation, TRM can be easily automated for investigating not only classical tectonic earthquakes but also long-period seismic events such as glacial earthquakes, tremors, seismic hum. We plan to apply it to any kind of seismic sources and particularly to environmental seismic sources.

ACKNOWLEDGMENTS

A number of colleagues and students have helped with suggestions for the improvement of this material. The work of Carene Larmat was partially funded by Institutional Support at Los Alamos National Laboratory, and Jean-Paul Montagner benefitted from an invitation from the Earthquake Research Institute of Tokyo and of the European ITN QUEST.

REFERENCES

Aki, K. & Richards, P., 1980. *Quantitative Seismology: Theory and Methods.,* Vol. I, W.H. Freeman and company, New York, NY.

Anderson, B.E., Griffa, M., Larmat, C., Ulrich, T. & Johnson, P.A., 2008. Time reversal, *Acoust. Today,* **4,** 5–16.

Campillo, M. & Paul, A., 2003. Long-range correlations in the diffuse seismic coda, *Science,* **299,** 547–549.

Capdeville, Y., 2005. An efficient born normal mode to compute sensitivity kernels and synthetic seismograms in the earth., *Geophys. J. Int.,* **163,** 1–8.

Capdeville, Y., Stutzmann, E. & Montagner, J.-P., 2000. Effects of a plume on long period surface waves computed with normal modes coupling., *Phys. Earth planet. Inter.,* **119,** 57–74.

Clévédé, E., Megnin, C., Lognonné, P. & Romanowicz, B., 2000. Seismic waveform modeling in a three-dimensional earth: asymptotic and non asymptotic approaches, *Phys. Earth planet. Int.,* **119,** 37–56.

Cohen-Tannoudji, C., Diu, B. & Lalo, F., 1973. *Mcanique quantique. 2 vols.,* Collection Enseignement des Sciences, ces, Paris. edn.

Debayle, E. & Sambridge, M., 2004. Inversion of massive surface wave datasets: model construction and resolution assessment, *J. geophys. Res.,* **109,** B02316, doi:10.1029/2003JB002652.

Derode, A., Tourin, A. & Fink, M., 1999. Ultrasonic pulse compression with one–bit time reversal through multiple scattering, *J. appl. Phys.,* **85**(9), 6343–6352.

Derode, A., Larose, E., Tanter, M., Campillo, M. & Fink, M., 2003. Recovering the Green's function from field–field correlations in an open scattering medium (l), *J. acoust. Soc. Am.,* **113**(6), 2973–2976.

Draeger, C. & Fink, M., 1997. One-channel time reversal of elastic waves in a 2D-Silicon Cavity, *Phys. Rev. Lett.,* **79**(3), 407–410.

Draeger, C. & Fink, M., 1999. One–channel Time Reversal in chaotic cavities: theoretical limits, *J. acoust. Soc. Am.,* **105**(2), 611–617.

Draeger, C., Aime, J.-C. & Fink, M., 1999. One-channel time-reversal in chaotic cavities: experimental results, *J. acoust. Soc. Am.,* **105**(2), 618–625.

Dziewonski, A. & Anderson, D., 1981. Preliminary reference earth model, *Phys. Earth planet. Int.,* **25,** 297–356.

Edmonds, A., 1960. *Angular Momentum and Quantum Mechanics,* Princeton University Press, Princeton, NJ.

Fink, M., 1996. Time reversal in acoustics, *Contemp. Phys.,* **37**(2), 95–109.

Fink, M., 1997. Time reversed acoustics, *Phys. Today,* **50**(3), 34–40.

Fink, M., 2006. Time reversal acoustics in geophysics, *Geophysics,* **71**(3), S151–S164.

Fink, M., Kuperman, W., Montagner, J.-P. & Tourin, A., 2002. *Imaging of Complex Media with Acoustic and Seismic Waves,* Topics in applied physics Vol. 82, Springer-Verlag, Berlin, 336pp.

Fukao, Y., Nishida, K., Suda, N., Nawa, K. & Kobayashi, N., 2002. A theory of earth's background free oscillations, *J. geophys. Res.,* **107,** B9, 2206, doi:10.1029/2001JB00153.

Gajewski, D. & Tessmer, E., 2005. Reverse modelling for seismic event characterization, *Geophys. J. Int.,* **163,** 276–284.

Gilbert, F., 1971. Excitation of the normal modes of the earth by earthquakes sources, *Geophys. J. R. astr. Soc.,* **22,** 223–226.

Halliday, D. & Curtis, A., 2008. Seismic interferometry, surface waves and source distribution, *Geophys. J. Int.,* **175**(3), 1067–1087.

Ishii, M., Shearer, P., Houston, H. & Vidale, J., 2005. Extent, duration and speed of the 2004 sumatra-andaman earthquake imaged by the hi-net array, *Nature,* **435,** 933–936.

Kawakatsu, H. & Montagner, J.-P., 2008. Time reversal seismic source imaging and moment-tensor inversion, *Geophys. J. Int,* **175,** 686–688.

Kim, Y., Liu, T. & Tromp, J., 2011. Adjoint centroid-moment tensor inversions, *Geophys. J. Int,* **186,** 264–278.

Kimman, W. P. & Trampert, J., 2010. Approximations in seismic interferometry and their effects on surface waves, *Geophys. J. Int.,* **182**(1), 461–476.

Kobayashi, N. & Nishida, K., 1998. Continuous excitation of planetary free oscillations by atmospheric disturbances, *Nature,* **395,** 357–360.

Komatitsch, D. & Vilotte, J.-P., 1998. The spectral element method: an efficient tool to simulate the seismic response of 3D and 3D geological structures, *Bull. seism. Soc. Am.,* **88,** 369–392.

Komatitsch, D., Ritsema, J. & Tromp, J., 2002. The spectral–element simulations, beowulf computing, and global seismology, *Science,* **298,** 1737–1742.

Kremers, S., Fichtner, A., Brietzke, G., Igel, H., Larmat, C., Huang, L. & Käser, M., 2011. Exploring the potentials and limitations of the time-reversal imaging of finite seismic sources, *Solid Earth,* **2,** 95–105.

Larmat, C., Montagner, J.-P., Fink, M., Capdeville, Y., Tourin, A. & Clévédé, E., 2006. Time-Reversal Imaging of seismic sources and application to the Great Sumatra Earthquake, *Geophys. Res. Lett.,* **33,** L19312, doi:10.1029/2006GL026336.

Larmat, C., Tromp, J., Liu, Q. & Montagner, J.-P., 2008. Time reversal location of glacial earthquakes, *J. geophys. Res.,* **113,** B09314, doi:10.1029/2008JB005607.

Larmat, C., Guyer, R. & Johnson, P., 2009. Tremor source location using time reversal, *Geophys. Res. Lett.,* **36,** L22034, doi:10.1029/2009GL040099.

Larmat, C., Guyer, R. & Johnson, P., 2010. Time reversal in geophysics, *Phys. Today,* **63,** 31–35.

Li, X.B. & Romanowicz, B., 1996. Global mantle shear-velocity model developed using nonlinear asymptotic coupling theory, *J. geophys. Res.,* **101**(B10), 22 245–22 272.

Li, X.-D. & Tanimoto, T., 1993. Waveforms of long-period body waves in a slightly aspherical earth, *Geophys. J. Int.,* **112,** 92–102.

Liu, T. & Tromp, J., 2008. Finite-frequency sensitivity kernels for global seismic wave propagation based upon adjoint methods, *Geophys. J. Int,* **174,** 265–286.

Downloaded from http://gji.oxfordjournals.org/ at INIST-CNRS on October 28,

Lobkis, O.I. & Weaver, R.L., 2001. On the emergence of the Green's function in the correlations of a diffuse field, *J. acoust. Soc. Am.,* **110**(6), 3011–3017.
McMechan, G., 1982. Determination of source parameters by wavefield extrapolation, *Geophys. J. Int.,* **71**(3), 613–628.
McMechan, G., Luetgert, J. & Mooney, W., 1985. Imaging of earthquake source in long valley caldera, california 1983, *Bull. seism. Soc. Am,* **75**(4), 1005–1020.
O'Brien, G., Lokmer, I., Barros, L.D., Bean, C., Saccorotti, G., Metaxian, J.-P. & Patane, D., 2011. Time reverse location of seismic long-period events recorded on Mt. Etna, *Geophys. J. Int.,* **184,** 452–462.
Phinney, R. & Burridge, R., 1973. Representation of the elastic-gravitationnal excitation of a spherical Earth model by generalized spherical harmonics, *Geophys. J. R. astr. Soc.,* **34,** 451–487.
Rhie, J. & Romanowicz, B., 2004. Excitation of Earth's continuous free oscillations by atmosphere–ocean–seafloor coupling, *Nature,* **431,** 552–556.
Romanowicz, B., 1987. Multiplet–multiplet coupling due to lateral heterogeneity: asymptotic effects on the amplitude and frequency of the Earth's normal modes., *Geophys. J. R. astr. Soc.,* **90,** 75–100.
Romanowicz, B., Panning, M., Gung, Y. & Capdeville, Y., 2008. On the computation of long period seismograms in a 3-D earth using normal mode based approximation, *Geophys. J. Int.,* **175,** 520–536.
Shapiro, N.M., Campillo, M., Stehly, L. & Ritzwoller, M., 2005. High-resolution Surface–wave tomography from ambient seismic noise, *Science,* **307,** 1615–1618.
Snieder, R., 2004. Extracting the green's function from the correlation of coda waves: a derivation based on stationary phase, *Phys. Rev.,* **E69,** 046610, doi:10.1103/PhysRevE.69.046610.
Suda, N., Nawa, K. & Fukao, Y., 1998. Earth's background free oscillations, *Science,* **279,** 2089–2091.
Tanimoto, T., 2008. Normal mode solution for the seismic noise cross-correlation method, *Geophys. J. Int.,* **175,** 1169–1175.
Tanimoto, T., Um, J., Nishida, K. & Kobayashi, N., 1998. Earths continuous oscillations observed in seismically quiet days, *Geophys. Res. Lett.,* **25,** 1553–1556.
Tarantola, A., 1988. Theoretical background for the inversion of seismic waveforms, Including Elasticity and Attenuation, *PAGEOPH,* **128**(1–2), 365–399.
Tromp, J., Tape, C. & Liu, Q., 2005. Seismic tomography, adjoint methods, time reversal and banana–doughnut kernels, *Geophys. J. Int.,* **160,** 195–216.
Tsai, V., 2010. The relationship between noise correlation and the green's function in the presence of degeneracy and the absence of equipartition, *Geophys. J. Int.,* **182,** 1509–1514.
Weaver, R. & Lobkis, O., 2002. On the emergence of the green's function in the correlations of a diffuse field: pulse echo using thermal photon, *Ultrasonics,* **40,** 435–439.
Woodhouse, J., 1980. The coupling and attenuation of nearly resonant multiplets in the earths free oscillation spectrum, *Geophys. J. astr. Soc.,* **61,** 261–283.
Woodhouse, J. & Girnius, T., 1982. Surface waves and free oscillations in a regionalized earth model, *Geophys. J. R. astr. Soc.,* **68,** 653–673.

APPENDIX A: BRA-KET FORMALISM AND NOTATIONS

This appendix reminds basic equations used in the manuscript and presents the Bra-Ket formalism routinely used in Quantum Mechanics. The elasto-dynamics (Navier-Stokes) equation for a continuum medium can be written in a condensed way

$$(\rho\partial_{tt} + H_0)\mathbf{u}(\mathbf{r}, t) = \mathbf{F}(\mathbf{r}, t), \tag{A1}$$

where H_0 is an integro-differential operator calculated in a reference Earth model. $\mathbf{F}$ expresses the ensemble of external forces applied in $\mathbf{r}$ at time t, and it is assumed that $\mathbf{F}$ is zero for $t < 0$. The vectorial eigenmode solutions of the eq. (A1) with a null external force are: $\mathbf{u}_K(\mathbf{r}, t) = |\mathbf{K}\rangle e^{-i\omega_K t}$, where ω_K are the eigenfrequencies and $|\mathbf{K}\rangle$ the eigenfunctions according to the Bra-Ket notation of quantum mechanics introduced by P. Dirac (see Cohen-Tannoudji *et al.* 1973). Kets $|\mathbf{K}\rangle$ are orthogonal, normalized vector functions, fulfilling the orthonormalization relationship

$$\langle\mathbf{K}'|\mathbf{K}\rangle = \int_V \rho\mathbf{u}^{\dagger}_{K'}(\mathbf{r}).\mathbf{u}_K(\mathbf{r})\,dV = \delta_{KK'}. \tag{A2}$$

The Bra $\langle\mathbf{K}|$ is the conjugate transpose (also called Hermitian conjugate $\mathbf{u}^{\dagger}_K$) of ket $|\mathbf{K}\rangle$. The reference Earth model might be 3-D but for sake of simplicity, it is usually considered as symmetric, non-rotating, purely elastic and transversely isotropic in hydrostatic state (SNREI model). For a SNREI model, the eigenmodes are characterized by three quantum numbers n, ℓ, m, eigenfrequencies are degenerate and are only dependent on n, ℓ. The eigenfunctions $|\mathbf{K}\rangle$ following the approach of Phinney & Burridge (1973), Woodhouse (1980) and Woodhouse & Girnius (1982) can be expressed by

$$\begin{aligned}|\mathbf{K}\rangle = |\mathbf{q}, \mathbf{n}, \mathbf{l}, \mathbf{m}\rangle &= {}_{\mathbf{n}}\mathbf{D}_\ell(r)Y_\ell^m(\theta,\phi) = \sum_{N=-1}^{N=1} {}_nD_\ell^N(r_R)Y_\ell^{Nm}(\theta_R,\phi_R)\hat{\mathbf{e}}^N \\ &= \left[{}_nU_\ell\mathbf{e}_r + \frac{1}{\sqrt{\ell(\ell+1)}}{}_nV_\ell\left(\mathbf{e}_\theta\frac{\partial}{\partial\theta} + \mathbf{e}_\phi\frac{1}{\sin\theta}\frac{\partial}{\partial\phi}\right) + \frac{1}{\sqrt{\ell(\ell+1)}}{}_nW_\ell\left(\mathbf{e}_\theta\frac{1}{\sin\theta}\frac{\partial}{\partial\phi} - \mathbf{e}_\phi\frac{\partial}{\partial\theta}\right)\right]Y_l^m(\theta,\phi) \\ &= \chi_\ell\Omega_0^\ell({}_nV_\ell - i\,{}_nW_\ell)Y_\ell^{-1m}\hat{\mathbf{e}}^- + \chi_\ell\,{}_nU_\ell Y_\ell^{0m}\hat{\mathbf{e}}^{\mathbf{0}} + \chi_\ell\Omega_0^\ell({}_nV_\ell + i\,{}_nW_\ell)Y_\ell^{1m}\hat{\mathbf{e}}^+,\end{aligned} \tag{A3}$$

where $\chi_\ell = \sqrt{\frac{2\ell+1}{4\pi}}$, $\Omega_0^\ell = \sqrt{\frac{(\ell-N+1)(\ell+N)}{2}}$, $\hat{\mathbf{e}}^N$ is one vector of the generalized complex-value basis $\{\hat{\mathbf{e}}^-, \hat{\mathbf{e}}^{\mathbf{0}}, \hat{\mathbf{e}}^+\}$ derived from the basis ($\mathbf{e}_r$, $\mathbf{e}_\theta$, $\mathbf{e}_\phi$) associated with spherical coordinates. $Y_\ell^{Nm}(\theta,\phi)$ are the generalized spherical harmonics of orders N, ℓ, m. The operator $D_k^N(r_R)$ is related to the eigenfunctions ${}_nU_\ell$, ${}_nV_\ell$, ${}_nW_\ell$ functions of radius r, only. The indices $K = (q, n, \ell, m)$ are: n (radial order), ℓ (angular order), m (azimuthal order), q takes the value 1 to indicate that the eigenmode is of spheroidal type (with associated eigenfunctions ${}_nU_\ell$, ${}_nV_\ell$), or two of toroidal type (with associated eigenfunctions ${}_nW_\ell$). The generalized spherical harmonics satisfy the orthogonality relation

$$\int_{-\pi}^{\pi}\int_0^{\pi} Y_{\ell'}^{Nm'*}(\theta,\phi)Y_\ell^{Nm}(\theta,\phi)\sin\theta\,d\theta\,d\phi = \frac{4\pi}{2\ell+1}\delta_{\ell\ell'}\delta_{mm'}. \tag{A4}$$

Downloaded from http://gji.oxfordjournals.org/ at INIST-CNRS on October 28, 2016

The integral of the inner product of two eigenvectors at the surface of the Earth is

$$\int_{-\pi}^{\pi}\int_{0}^{\pi} {}_{n'}\mathbf{u}_{\ell'}^{m\dagger}(r,\theta,\phi).{}_{n}\mathbf{u}_{\ell}^{m}(r,\theta,\phi)\sin\theta d\theta d\phi = \chi_{\ell}^{2}(2\Omega_{0}^{\ell^2}(V+W)^2+U^2)\frac{4\pi}{2\ell+1}. \tag{A5}$$

We will note in the following ${}_{n}D_{\ell}^{2}(r) = \frac{4\pi\chi_{\ell}^{2}}{2\ell+1}\{2\Omega_{0}^{\ell^2}[V(r)+W(r)]^2+U(r)^2\}$ and we omit the indices n and ℓ for the functions U, V, W.

A very useful theorem is the addition theorem (also named closure relationship)

$$\sum_{K}|\mathbf{K}(\mathbf{r})\rangle\langle\mathbf{K}(\mathbf{r}')| = \Sigma_{K}\mathbf{u}_{\mathbf{K}}(\mathbf{r})\mathbf{u}_{\mathbf{K}}^{\dagger}(\mathbf{r}') = \mathbf{I}\delta(\mathbf{r}-\mathbf{r}'), \tag{A6}$$

where $\mathbf{I}$ is the identity matrix. When using classical spherical harmonics $Y_{\ell}^{m}(\theta,\phi)$, the following addition theorem expression is found

$$\sum_{m=-\ell}^{m=\ell} Y_{\ell}^{m*}(\theta_E,\phi_E)Y_{\ell}^{m}(\theta_R,\phi_R) = \frac{2\ell+1}{4\pi}P_{\ell}^{0}(\cos\Delta_{ER}), \tag{A7}$$

where Δ_{ER} is the angular distance between E and R. There are some other useful relationships, such as generalization of classical addition theorem (see e.g. Li & Romanowicz 1996; Capdeville *et al.* 2000), applied to generalized spherical harmonics $Y_{\ell}^{Nm}(\theta,\phi)$ (Edmonds 1960; Phinney & Burridge 1973)

$$\sum_{m=-\ell}^{m=\ell} Y_{\ell}^{N'm*}(\theta_E,\phi_E)Y_{\ell}^{Nm}(\theta_R,\phi_R) = \frac{2\ell+1}{4\pi}e^{iN'\gamma_{ER}}P_{\ell}^{NN'}(\cos\Delta_{ER})e^{iN\alpha_{ER}}, \tag{A8}$$

where $P_{\ell}^{NN'}(\cos\Delta_{ER})$ are the generalized Legendre functions. The index ${}_{E}$ is related to the source location, and the index ${}_{R}$ to the receiver location. The angle $-\alpha_{ER}$ is the backazimuth at the receiver, $\pi-\gamma_{ER}$ is the azimuth at the source, and Δ_{ER} is the epicentral distance between the source E and the receiver R (see Fig. 1). Another property of the eigenmodes written in the Bra-Ket notation, in which the operator H_0 intervenes, is

$$\langle\mathbf{K}'(\mathbf{r}')|H_0|\mathbf{K}(\mathbf{r})\rangle = \int_{V}dV\int_{V'}dV'\,\mathbf{u}_{\mathbf{K}'}^{\dagger}(\mathbf{r}')H_0\mathbf{u}_{\mathbf{K}}(\mathbf{r}) = \omega_{K}^{2}\delta_{KK'}. \tag{A9}$$

All displacement solutions of (A1) can be expanded into the set of eigenmodes

$$\mathbf{u}(\mathbf{r},t) = \sum_{K}a_{K}\mathbf{u}_{K}(\mathbf{r})e^{-i\omega_{K}t} = \sum_{K}a_{K}|\mathbf{K}\rangle e^{-i\omega_{K}t}, \tag{A10}$$

where a_K are the excitation coefficients of mode K depending on the location and characteristics of the source with the system of forces $\mathbf{F}$ (developed at the end of this section). At first, some useful notations can be introduced, such as the dot product, $\mathbf{u}.\mathbf{v} = \sum_i u_i.v_i$ and the inner product

$$\langle\mathbf{u}|\mathbf{v}\rangle = \int_{V}\rho\mathbf{u}^{\dagger}(r).\mathbf{v}(r)\,dV, \tag{A11}$$

where V is the whole Earth volume. The excitation coefficient a_K of eq. (A10) is usually calculated in the frequency domain by taking either the Fourier or the Laplace transform (Gilbert 1971) of eq. (A1). In the frequency domain, the displacement produced at the position $\mathbf{r}_R$ by a body force distribution $\mathbf{F}(\mathbf{r}_E,\omega)$ is

$$\mathbf{u}(\mathbf{r}_{\mathbf{R}},\omega) = \sum_{K}\left[\int_{V_E}dV\,\mathbf{u}_{\mathbf{K}}^{\dagger}(\mathbf{r}_{\mathbf{E}})\mathbf{F}(\mathbf{r}_{\mathbf{E}},\omega)\right]\frac{\mathbf{u}_{\mathbf{K}}(\mathbf{r}_{\mathbf{R}})}{-\omega^2+\omega_{K}^{2}} = \sum_{K}|\mathbf{K}_{\mathbf{R}}\rangle\langle\mathbf{K}_{\mathbf{E}}|\mathbf{F}_{\mathbf{E}}(\omega)\rangle\frac{1}{-\omega^2+\omega_{K}^{2}}, \tag{A12}$$

where we note $|\mathbf{K}_{\mathbf{E}}\rangle = |\mathbf{K}(\mathbf{r}_{\mathbf{E}})\rangle = \mathbf{u}_{\mathbf{K}}(\mathbf{r}_{\mathbf{E}})\delta(\mathbf{r}-\mathbf{r}_{\mathbf{E}})$, $|\mathbf{K}_{\mathbf{R}}\rangle = |\mathbf{K}(\mathbf{r}_{\mathbf{R}})\rangle = \mathbf{u}_{\mathbf{K}}(\mathbf{r}_{\mathbf{R}})\delta(\mathbf{r}-\mathbf{r}_{\mathbf{R}})$. The same notation will be used later on for other points. An inverse Fourier transform can be performed to come back in the time domain. We will consider two cases for the source time function, a dirac in time, $\delta(t)$ and a Heaviside function, $H(t)$, also known as 'step function', which is more realistic for an earthquake. For a dirac source time function

$$\mathbf{u}(\mathbf{r}_{\mathrm{R}},t) = \sum_{K}\mathbf{u}_{\mathbf{K}}(\mathbf{r}_{\mathbf{R}})\int_{V_E}dV\,\mathbf{u}_{\mathbf{K}}^{\dagger}(\mathbf{r}_{\mathbf{E}})\mathbf{F}_0(\mathbf{r}_E)\,H(t)\frac{\sin(\omega_K t)}{\omega_K} = \sum_{K}|\mathbf{K}_{\mathbf{R}}\rangle\langle\mathbf{K}_{\mathbf{E}}|\mathbf{F}_{\mathbf{E}}\rangle H(t)\frac{\sin(\omega_K t)}{\omega_K} \tag{A13}$$

The Green's function $\mathbf{G}(\mathbf{r}_{\mathbf{E}},\mathbf{r}_{\mathbf{R}},t;0)$ is simply given by

$$\mathbf{G}(\mathbf{r}_{\mathbf{E}},\mathbf{r}_{\mathbf{R}},t;0) = \sum_{K}|\mathbf{K}_{\mathbf{R}}\rangle\langle\mathbf{K}_{\mathbf{E}}|\;H(t)\frac{\sin(\omega_K t)}{\omega_K}. \tag{A14}$$

For acoustic waves (scalar waves), the Green's function is a scalar function, whereas for elastic waves, it is a second-order tensor. Let us index the three components of vectors by γ at the source point E, by β at point R, and by α for any other point M that will be introduced later. The β component of the Green's function which is the response of an impulse $[F^{\gamma}(\mathbf{r},t) = F_0^{\gamma}\delta(\mathbf{r}-\mathbf{r}_E)\delta(t)]$ applied at a source point $\mathbf{r}_E$, is

$$G^{\beta\gamma}(\mathbf{r}_{\mathbf{E}},\mathbf{r}_{\mathbf{R}},t;0) = \sum_{K}u_{K}^{\beta}(\mathbf{r}_R)u_{K}^{\gamma\star}(\mathbf{r}_E)H(t)\frac{\sin(\omega_K t)}{\omega_K} = \sum_{K}|\mathbf{K}_{\mathbf{R}}^{\beta}\rangle\langle\mathbf{K}_{\mathbf{E}}^{\gamma}|w(t), \tag{A15}$$

where $w(t) = H(t)\frac{sin(\omega_K t)}{\omega_K}$. The spatial reciprocity $\mathbf{G}_{ER}^{\gamma\beta} = \mathbf{G}_{RE}^{\beta\gamma}$ is straightforward for the real part of the Green's function from eqs (A14) and (A15), but it must be noted that it is more complex than for scalar waves. For a point source Heaviside function in time, it is usual to

Downloaded from http://gji.oxfordjournals.org/ at INIST-CNRS on October 28,

introduce the seismic moment tensor $M_{\zeta\gamma}$ (see e.g. Aki & Richards 1980) such that $F_0^{\gamma}(\mathbf{r_E}) = -M_{\gamma\zeta}\frac{\partial}{\partial\xi_\zeta}\delta(\xi - \mathbf{r_E})$, and the deformation tensor $\epsilon^K_{\gamma\zeta}$. The general expression of displacement is given by

$$\mathbf{u}(\mathbf{r}_R, t) = \sum_K \mathbf{u}_K(\mathbf{r}_R)\sum_{\gamma\zeta}\epsilon^{K\star}_{\gamma\zeta}(\mathbf{r}_E)M_{\gamma\zeta}H(t)\frac{1-\cos(\omega_K t)}{\omega_K^2} = \sum_K |\mathbf{K_R}\rangle\langle\mathbf{K_E}|\mathbf{E}\mathbf{M}w'(t), \tag{A16}$$

where $w'(t) = H(t)\frac{-\cos(\omega_K t)}{\omega_K^2}$. This expression found by Gilbert (1971), is used on a routine basis for calculating synthetic seismograms. It can be shown that the contribution of all eigenmodes tends to cancel out except when there is a constructive interference between modes corresponding to a stationary phase (Romanowicz 1987). The eq. (A16) can be easily related to the previous expression (A13), for $t > 0$, by taking the time derivative of $\mathbf{u}(\mathbf{r}_R, t)$, the velocity of the field. For $t > 0$, the second time derivative corresponding to the acceleration $\Gamma(\mathbf{r}_R, t)$ has a very simple expression

$$\Gamma(\mathbf{r}_R, t) = \sum_K \mathbf{u}_K(\mathbf{r}_R)\cos(\omega_K t)\int_{V_E} dV_E \mathbf{u}_K^{\dagger}(\mathbf{r}_E).\mathbf{F}_0(\mathbf{r}_E). \tag{A17}$$

So, in both cases of source time function, the Green's function can be easily calculated by normal mode summation.

APPENDIX B: THE OBSERVATION POINT M IS AT THE SOURCE POINT E: CAVITY EQUATION

The time reversal of acoustic waves (scalar case) by mode theory has been extensively investigated in Draeger & Fink (1999). In the acoustic case, $\mathbf{F}_E$ is reduced to a scalar value F_E, and there is no difference for scalar eigenfunctions between bra and ket. Draeger & Fink (1999) obtained the remarkable cavity equation for acoustic waves when the observation point M is located at the source point E

$$G_{RR}(t) * F_E.G_{EE}(-t) = G_{RE}(t) * F_E.G_{ER}(-t) = \sum_K \frac{F_E}{{\omega_K}^2}u_K(R)^2\, u_K(E)^2\frac{1}{2}\Delta\tau\cos\omega_K t. \tag{B1}$$

The Green's functions G_{EE} and G_{RR} are the backscattering impulse response at points R and E. So the time-reversal field $S_E(t)$ at point E is the convolution of these two backscattering impulse responses $G_{EE}(-t)$ by $G_{RR}(t)$. We wonder whether this property is still valid in the 3-D elastic case. In the case $J = K$ and $M = E$, eq. (11) valid for acoustic and elastic cases, becomes at point E

$$S_E(t) = \sum_K \frac{1}{\omega_K^2}|\mathbf{K_E}\rangle\langle\mathbf{K_R}|\mathbf{K_R}\rangle\langle\mathbf{K_E}|\mathbf{F_E}\rangle\frac{1}{2}\Delta\tau\cos\omega_K t. \tag{B2}$$

In the general elastic case,

$$\begin{aligned}
\mathbf{F_E}.\mathbf{G_{EE}}(t) &= \sum_K \frac{1}{\omega_K}|\mathbf{K_E}\rangle\langle\mathbf{K_E}|\mathbf{F_E}\rangle\sin\omega_K t,\\
\mathbf{G_{RR}}(t) &= \sum_J \frac{1}{\omega_J}|\mathbf{J_R}\rangle\langle\mathbf{J_R}|\sin\omega_J t,\\
\mathbf{G_{RR}}(t) * \mathbf{F_E}.\mathbf{G_{EE}}(-t) &= \sum_J\sum_K \frac{1}{\omega_J}|\mathbf{J_R}\rangle\langle\mathbf{J_R}|\frac{1}{\omega_K}|\mathbf{K_E}\rangle\langle\mathbf{K_E}|\mathbf{F_E}\rangle\Im_{JK}(t),
\end{aligned} \tag{B3}$$

where $\Im_{JK}(t)$ is the same integral introduced in eq. (8). Since there is no difference for scalar eigenfunctions between bra and ket, the eqs (B2) and (B3) are, as expected, equivalent for $J = K$ in the acoustic case.

In the elastic case, the cavity equation is no longer valid. The equivalent of the cavity equation is more complex, since it is necessary to take account of the tensorial character of Green's functions and of the difference between bra and ket. If only the dominant diagonal elements of $\Im_{JK}(t)$ are taken into account,

$$\mathbf{G_{RE}}(t) * \mathbf{F_E}.\mathbf{G_{ER}}(-t) = \sum_K |\mathbf{K_E}\rangle\langle\mathbf{K_R}|\mathbf{K_R}\rangle\langle\mathbf{K_E}|\mathbf{F_E}\rangle\frac{\Im_{KK}}{\omega_K^2} \tag{B4}$$

and

$$\mathbf{G_{RR}}(t) * \mathbf{F_E}.\mathbf{G_{EE}}(-\mathbf{t}) = \sum_K |\mathbf{K_R}\rangle\langle\mathbf{K_R}|\mathbf{K_E}\rangle\langle\mathbf{K_E}|\mathbf{F_E}\rangle\frac{\Im_{KK}}{\omega_K^2}. \tag{B5}$$

So it is easily seen that $|\mathbf{K_R}\rangle\langle\mathbf{K_R}|\mathbf{K_E}\rangle\langle\mathbf{K_E}| \neq |\mathbf{K_E}\rangle\langle\mathbf{K_R}|\mathbf{K_R}\rangle\langle\mathbf{K_E}|$. Actually, the scalar product $\langle\mathbf{K_R}|\mathbf{K_R}\rangle$ appears in eq. (B4) whereas it is the scalar product $\langle\mathbf{K_R}|\mathbf{K_E}\rangle$ which comes up in eq. (B5). However, if we project both expressions in eqs (B4) and (B5) on $\langle\mathbf{K_R}|$, the same expression is obtained, $\langle\mathbf{K_R}|\mathbf{K_E}\rangle\langle\mathbf{K_R}|\mathbf{K_R}\rangle\langle\mathbf{K_E}|\mathbf{F_E}\rangle\frac{\Im_{KK}}{\omega_K^2}$. In the elastic case, the cavity equation is no longer valid, but an equivalent of the cavity equation has been derived by projecting both terms of eqs (B4) and (B5) on the basis vector $\langle\mathbf{K_R}|$.

Downloaded from http://gji.oxfordjournals.org/ at INIST-CNRS on October 28, 2016